ACS OMEGA

Open Access

http://pubs.acs.org/journal/acsodf

Article

Enhancing Cardiomyocyte Resilience to Ischemia-Reperfusion Injury: The Therapeutic Potential of an Indole-Peptide-Tempo Conjugate (IPTC)

Shanshan Hou, Xin Yan, Xiang Gao, Steffen Jockusch, K. Michael Gibson, Zhiying Shan,* and Lanrong Bi*

Cite This: *ACS Omega* 2024, 9, 39401−39418

Read Online

ACCESS | Metrics & More | Article Recommendations

ABSTRACT: Ischemia/reperfusion (I/R) injury leads to apoptosis and extensive cellular and mitochondrial damage, triggered by the early generation and subsequent accumulation of mitochondrial reactive oxygen species (mtROS). This condition not only contributes to the pathology of I/R injury itself but is also implicated in a variety of other diseases, especially within the cardiovascular domain. Addressing mitochondrial oxidative stress thus emerges as a critical therapeutic target. In this context, our study introduces an indole-peptide-tempo conjugate (IPTC), a compound designed with dual functionalities: antioxidative properties and the ability to modulate autophagy. Our findings reveal that IPTC effectively shields H9C2 cardiomyocytes against hypoxia/reoxygenation (H/R) damage, primarily through counteracting mtROS overproduction linked to impaired mitophagy and mitochondrial dysfunction. We propose that IPTC operates by simultaneously reducing mtROS levels and inducing mitophagy, highlighting its potential as a novel therapeutic strategy for mitigating mitochondrial oxidative damage and, by extension, easing I/R injury and potentially other related cardiovascular conditions.

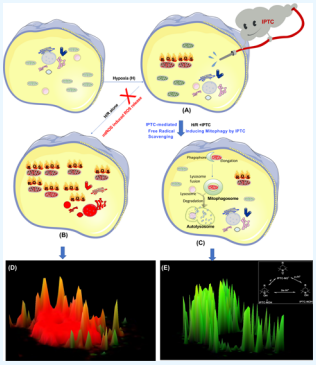

1. INTRODUCTION

Ischemia/reperfusion (I/R) injury is a complex pathophysiological event that occurs when the blood supply to an organ or tissue is temporarily disrupted and restored, leading to cellular and tissue damage.[1,2] This phenomenon plays a pivotal role in various medical conditions, including myocardial infarction,[3] stroke,[4] organ transplantation,[5] and surgical procedures involving temporary blood flow cessation. Understanding the mechanisms underlying I/R injury is crucial for developing effective interventions to mitigate its adverse effects.

During the ischemic phase, reduced blood flow deprives tissues of oxygen and nutrients, resulting in metabolic shifts and cellular damage. Upon reperfusion, tissue damage is exacerbated due to oxidative stress,[6] inflammation,[7] endothelial dysfunction,[8] mitochondrial damage,[6] dysregulated autophagy, and apoptosis.[9] These pathological processes contribute to further cellular injury and impede tissue recovery.

Numerous therapeutic approaches have been explored to address the multifaceted nature of I/R injury, including antioxidants,[10−13] anti-inflammatory agents, and techniques such as ischemic preconditioning and postconditioning.[14−16] Despite advances, effectively managing I/R injury remains challenging, necessitating ongoing research and innovative treatment strategies.

Indole derivatives have captured the scientific community's attention for their vast array of biological activities, including their potential as anti-inflammatory, antioxidant, and autophagy-modulating agents.[17−31] With their unique and versatile chemical structure, these compounds present a promising avenue for treating I/R injury. I/R injury involves a complex series of cellular damage mechanisms triggered when blood supply is reinstated to ischemic tissues, leading to further tissue damage rather than recovery.

The potent anti-inflammatory properties of indole derivatives play a pivotal role in I/R injury,[17−31] where the inflammatory response initiated by reperfusion significantly contributes to subsequent tissue damage. The cascade of cytokines and chemokines released by endothelial cells and the infiltration of leukocytes into the ischemic tissue aggravate the condition, leading to enhanced tissue permeability, edema, and further cellular death.[1,2] By modulating these inflammatory pathways and inhibiting the production and activity of pro-inflammatory cytokines such as TNF-α, IL-1β, and IL-6, indole derivatives can curtail the infiltration of inflammatory cells, thereby reducing the overall extent of damage and facilitating tissue recovery. Alongside inflammation, the surge of reactive

Received: March 20, 2024
Revised: June 18, 2024
Accepted: June 20, 2024
Published: September 13, 2024

oxygen species (ROS) during reperfusion is critical in exacerbating I/R injury.[4,7] These ROS cause lipid peroxidation and DNA damage and provoke further inflammation, intensifying the injury.[4,7] Indole derivatives counteract this by showcasing remarkable antioxidant properties that scavenge harmful free radicals and bolster cellular antioxidant defenses.[17−31] This reduction in oxidative stress helps protect the integrity and function of cellular components, highlighting the dual protective mechanism of indole derivatives against the destructive events of I/R injury.

Furthermore, indole derivatives influence autophagy, a cellular mechanism that removes damaged organelles and proteins.[22,32−34] Autophagy's role in I/R injury is dual-sided; while excessive autophagy can lead to cell death, a controlled level is protective, clearing damaged mitochondria and preventing protein accumulation.[22] Indole derivatives promote these protective roles of autophagy, aiding in maintaining cellular homeostasis and inhibiting injury progression.[32,35−37] This autophagy-modulating capability, combined with their antioxidant and anti-inflammatory actions, position indole derivatives as comprehensive therapeutic agents against I/R injury.[22,32−37]

The inherent versatility of the indole structure in medicinal chemistry adds another layer of appeal. Central to this appeal is its aromaticity, stemming from the resonance of π electrons across the benzene and pyrrole rings. This aromatic character not only bestows stability upon the molecule but also dictates its reactivity and pharmacological behaviors.[38,39] Such inherent aromaticity renders indole amenable to diverse functionalizations, paving the way for synthesizing an extensive array of derivatives tailored to specific pharmacological profiles.

Its electrophilic sites underpin the reactivity of indole, notably the C2 and C3 positions, where nucleophilic substitution is particularly pronounced owing to the lone pair electrons on the nitrogen atom and its adjacent carbon, respectively. Manipulation at these sites profoundly alters indole derivatives' physicochemical and pharmacological attributes. Meanwhile, the basicity conferred by the nitrogen atom in the pyrrole ring influences the interaction of indole compounds with biological targets, offering a lever for modulating pharmacological behavior through targeted modifications.[38,39]

Indole's functionalization landscape is vast, permitting the introduction of diverse substituents at multiple positions along its scaffold. From nitrogen atom (N1) to various carbon positions on the benzene and pyrrole rings, substitutions offer avenues for enhancing potency, improving pharmacokinetics, and refining selectivity. Such strategic modifications capitalize on steric effects, with the three-dimensional arrangement of substituents critically impacting interactions with biological targets. Conformational flexibility further augments this interplay, affording varied spatial arrangements that influence bioavailability, membrane permeability, and molecular interactions.

Moreover, the capacity for indole derivatives to engage in hydrogen bonding underpins their binding to target proteins or receptors, orchestrating specific molecular interactions pivotal for biological activity. Understanding these structural intricacies empowers the rational design and optimization of indole-based therapeutics for diverse ailments, including I/R injury. Researchers can navigate the complexities of drug development by leveraging the innate versatility of the indole structure, forging novel compounds endowed with heightened efficacy, refined selectivity, and enhanced safety profiles.

Over the past decade, our research team has focused on synthesizing various indole derivatives to address I/R injury.[18−31] With a primary goal of advancing I/R injury treatment, we've prioritized developing and investigating new indole derivatives, creating a series of indole-peptide-tempol conjugates. The indole alkaloid scaffold is at the core of our strategy, selected for its diverse biological activities, including anti-inflammatory, antioxidant, and neuroprotective effects. Utilizing this scaffold as a versatile foundation, our objective has been to adjust it to target defective autophagy and oxidative stress finely, both central to I/R injury.

Moreover, we've incorporated the RGD peptide motif to interact with integrins, which is crucial for cell interactions.[18,40−42] We aim to subtly influence critical cellular functions such as adhesion, migration, and survival relevant to I/R injury. By strategically modulating integrin signaling to impact autophagy and apoptosis, we aim to support cell survival in stressed or damaged tissues.

Additionally, including the Tempol component enhances antioxidant capabilities in our conjugates, explicitly targeting the extensive ROS present during the reperfusion phase of I/R injury. By combining these three elements into a single molecule, we strive to offer a comprehensive therapeutic approach. While our approach is still in its early stages, the significant antioxidant and autophagy-promoting activity observed in IPTC holds promise for the potential efficacy of our intervention. This manuscript provides detailed insights into the design, synthesis, and initial biological evaluation of IPTC.

2. MATERIALS AND METHODS

2.1. Synthesis of IPTC. *2.1.1. Synthesis of (1S,3S)-1-Methyl-2,3,4,9-tetrahydro-1H-pyrido[3,4-b]indole-3-carboxylic Acid (1).* To a solution of 0.5 mL 98% H_2SO_4 in distilled water (200 mL), L-Trp (5g, 25 mmol) was added in three portions. The mixture was stirred at r.t. for 15 min, and then CH3CHO (5 mL) was added dropwise. The reaction mixture continued stirring at r.t. overnight until the precipitate appeared. Then, concentrated ammonia solution (∼1.5 mL) was added to adjust the pH to 7.0. The formed precipitate was collected by filtration (78% yield). Mp 287−289 °C. ESI/MS 231 $[M + H]^+$. IR (KBr) 3101−2405, 2962, 2905, 1703, 1624, 1595, 1506, 1453, 1376, 1072, 904 cm^{-1}.^{1}H NMR (400 MHz, DMSO-d_6) d/ppm = 11. 92 (s, 1 H), 10. 97 (s, 1 H), 9.17 (s, 1 H), 7. 45 (d, J = 7.5 Hz, 1 H), 7. 36 (t, J = 8.0 Hz, 1 H), 7.10 (t, J = 8.0 Hz, 1 H), 7.01 (t, J = 7.5 Hz, 1 H), 4.22 (q, J = 4.8 Hz, 1H), 3.66 (dd, J = 10.5 Hz, J = 5.0 Hz, 1 H), 3.14 (dd, J = 10. 5 Hz, J = 2.4 Hz, 1 H), 2. 85 (ddd, J = 10.5 Hz, J = 5.0 Hz, J = 2.4 Hz, 1 H), 1. 38 (d, J = 5.0 Hz, 3 H).

2.1.2. Synthesis of Methyl-1-methyl-1,2,3,4-tetrahydro-β-carboline-3-carboxylate (2). At 0 °C, to 10 mL methanol, 1 mL of thionyl chloride was added dropwise. The mixture was stirred at r.t. for 15 min, and then 2.0 g (8.7 mmol) of 1-methyl-1,2,3,4-tetrahydro-β-carboline-3-carboxylic acid 1 was added slowly. The reaction mixture was stirred at r.t. until TLC ($CHCl_3$/MeOH, 15:1) indicated the complete disappearance of 1-methyl-1,2,3,4-tetrahydro-β-carboline-3-carboxylic acid. The reaction mixture was neutralized with an aqueous sodium bicarbonate solution (10%) to pH 7.0. The formed precipitate was collected by filtration (82% yield). ESI/MS: 245 [M + H].

https://doi.org/10.1021/acsomega.4c02725
ACS Omega 2024, 9, 39401−39418

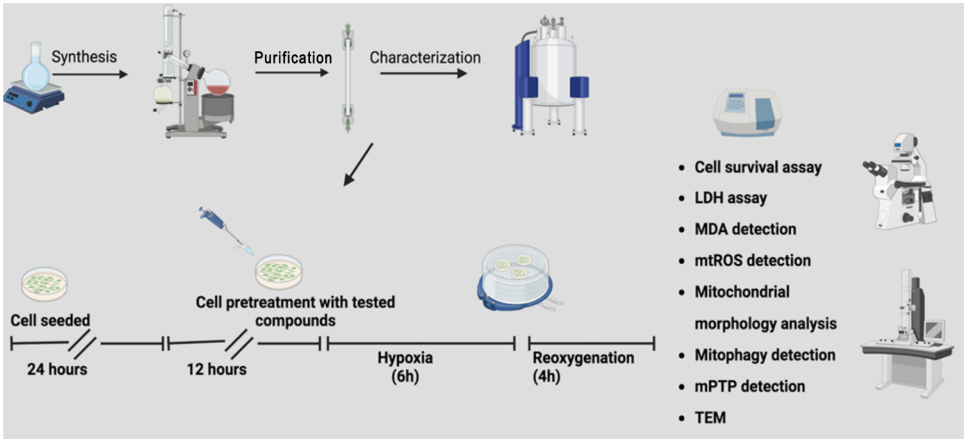

Figure 1. Several complementary assays are used to assess the impact of IPTC on mitochondrial function (Created with BioRender.com).

*2.1.3. Synthesis of Methyl-1-methyl-β-carboline-3-carboxylate (**3**).* A suspension of 5.0 g (20.0 mmol) of compound **2**, 1.4 g (20. mmol) sulfur flour, and 20 mL of anhydrous dimethylbenzene was refluxed until TLC ($CHCl_3$/MeOH, 15:1) indicated the complete disappearance of compound **2**. On evaporation, the residue was dissolved in 10 mL of MeOH. After filtration and evaporation under reduced pressure, 3.2 g (65%) of compound 3 was obtained as a yellow powder. Mp 242−243 °C; ESI/MS: 241 [M + H]+; IR (KBr): 3310, 2954, 2922, 2901, 2811, 1742, 1600, 1581, 1566, 1450, 1380, 1066, 900 cm^{-1}; ^1H NMR (400 MHz, DMSO-d_6): δ = 9.98 (s, 1H), 7.41 (d, J = 5.6 Hz, 1H), 7.35 (d, J = 7.2 Hz, 1H), 7.15 (d, J = 8.2 Hz, 1H), 7.11 (t, J = 7.5 Hz, 1H), 6.97 (t, J = 6.4 Hz, 1H), 3.74 (s, 3H), 2.03 (s, 3H).

*2.1.4. Synthesis of 1-Methyl-β-carboline-3-carboxylic Acid (**4**).* To a solution of 5.0 g (20.8 mmol) of compound (**3**), 120 mL of the aqueous solution of sodium hydroxide (2.0 mmol/L) was added and then stirred at 60 °C until TLC ($CHCl_3$/MeOH, 15:1) indicated the complete disappearance of compound (**3**). The reaction mixture was neutralized with hydrochloric acid to pH 7.0. The formed precipitate was collected by filtration to give 3.86 g (82%) of compound 4 as a yellow powder. Mp 292−293 °C; ESI/MS: 227 [M + H]$^+$; IR (KBr): 3230, 2252, 2924, 2910, 2900, 1700, 1610, 1585, 1562, 1440, 1380, 1066, 900 cm^{-1}; ^1H NMR ($CDCl_3$): δ = 11.06 (s, 1H), 9.88 (s, 1H), 7.42 (d, J = 5.8 Hz, 1H), 7.39 (d, J = 7.1 Hz, 1H), 7.10 (d, J = 8.0 Hz, 1H), 7.10 (t, J = 7.6 Hz, 1H), 6.99 (t, J = 6.6 Hz, 1H), 2.10 (s, 3H).

*2.1.5. Synthesis of Compound **6**.* 0.20 mmol of hydroxybenzotriazole (HOBt) and 0.25 mmol of dicyclohexylcarbodiimide (DCC) were added to a solution containing 0.20 mmol of compound **4** in 5 mL of anhydrous THF at 0 °C. The reaction mixture was stirred at 0 °C for 24 h. Precipitated dicyclohexylurea was isolated by filtration. The filtrate was evaporated under reduced pressure, and the residue was triturated with petroleum ether to provide the corresponding ester. 0.20 mmol of tetrapeptide (**5**) and 0.26 mmol of *N*-methylmorpholine were added to a solution of the preceding ester in 10 mL of anhydrous THF. The reaction mixture was stirred at room temperature for 24 h. Following evaporation, the residue was dissolved in 50 mL of ethyl acetate. The solution was washed with 5% sodium bicarbonate, followed by 5% citric acid and saturated sodium chloride, and the organic phase was separated and dried over anhydrous sodium sulfate. Following filtration and evaporation under reduced pressure, compound **6** was obtained by column chromatography purification ($CHCl_3$/CH_3OH, 30:1). Mp 103−104 °C; $[\alpha]_D^{25}$ = −2.38 (c = 0.375, CH_3OH + DMF); ESI/MS: 958 [M + H]$^+$; IR (KBr) 3305, 3064, 3034, 2933, 2872, 1737, 1654, 1625, 1597, 1527, 1498, 1452, 1388, 1352, 1261, 1251, 1215, 1151, 1105, 1001, 908, 785, 738, 698, 582, 516 cm^{-1}.^1H NMR (DMSO, 400 MHz) δ/ppm = 11.96 (s, l H), 8.69 (m, 2 H), 8.52 (m, l H), 8.45 (d, J = 7.8 Hz, l H), 8.32 (d, J = 7.5 Hz, 2 H), 8.18−7.50 (m, 2 H), 7.67−7.56 (m, 2 H), 7.33−7.24 (m, 16 H), 5.16−5.10 (m, 2H), 5.06−5.01 (m, 2 H), 4.82 (q, J = 8.1 Hz, l H), 4.68 (q, J = 7.8 Hz, l H), 4.59 (q, J = 4.8 Hz, l H), 4.45 (q, J = 12 Hz, 2 H), 4.02−3.75 (m, 3 H), 3.70−3.63 (m, l H), 3.20 (m, 2 H), 3.02−2.83 (m, 3 H), 2. 78−2.73 (m, 2 H), 2.67−2.59 (m, l H), 1.85−1.81 (m, l H), 1.78−1.74 (m, l H), 1.57 (m, 2 H); ^{13}C NMR (DMSO, 75 MHz) δ/ppm = 172.25, 171.05, 170.25, 170.15, 169.21, 169.11, 164.98, 159.77, 141.51, 141.34, 138.90, 138.25, 136.50, 136.46, 136.22, 136.15, 128.80, 128.63, 128.48, 128.42, 128.38, 128.34, 128.27, 128.13, 127.95, 127.91, 127.06, 126.88, 122.53, 121.91, 120.45, 112.76, 112.71, 72.74, 69.48, 66.59, 66.15, 53.15, 52.46, 49.53, 42.40, 36.81, 30.83, 25.25, 20.91.

*2.1.6. Synthesis of Compound **7**.* 0.2 mmol of compound 6 was added to 1 mL of phenyl methyl ether, 1 mL of dimethyl sulfide, and 4 mL of HF and stirred at 0 °C for 2 h. The reaction mixture was evaporated under reduced pressure and the residue was then triturated with petroleum ether. The triturated residue was further purified on Sephadex G-10, followed by HPLC purification (56% yield). Mp 78−79 °C. $[\alpha]_D^{25}$ = −6.64 (c = 0.5, H_2O). ESI/MS: 642 [M + H]$^+$; IR (KBr) 3278, 3199, 2785, 2318, 1668, 1533, 1465, 1400, 1278, 1255, 1170, 1114, 1031, 896, 866, 667, 640, 576, 518, 457 cm^{-1}; ^1H-NMR (DMSO, 400 MHz) δ/ppm = 12.03 (s, l H), 8.70 (m, 2 H), 8.34 (d, J = 7.8 Hz, l H), 7.74 (m, l H), 7.66−7.56 (m, 3 H), 7.31−7.26 (m, 4 H), 4.65 (m, l H), 4.58 (m, 2 H), 4.15 (m, 2 H), 3.88−3.58 (m, 4 H), 3.15−3.07 (m, 2 H), 2.85 (m, 3 H), 2.71 (m, l H), 2.58 (m, l H), 2.45 (m, 3 H), 1.94 (m, l H), 1.77 (m, l H), 1.56 (m, 2 H). ^{13}C-NMR (DMSO, 75 MHz) δ/ppm = 172.80, 172.46, 171.07, 169.03, 164.93, 157.31, 141.55, 141.34, 138.83, 136.50, 128.83, 127.88, 123.30, 122.57, 121.87, 120.46, 119.03, 112.74, 65.14, 61.89, 54.21, 49.86, 44.67, 42.52, 36.99, 30.86, 25. 30, 20.95.

2.1.7. Synthesis of IPTC. At 0 °C, 4-amino Tempo (1.6 mmol), and a catalytic amount of HOBt were added to a solution of compound 7 (1.5 mmol) in CH_2Cl_2, 1-ethyl-3-(3-(dimethylamino)propyl) carbodiimide (EDC) (1.6 mmol).

https://doi.org/10.1021/acsomega.4c02725
ACS Omega 2024, 9, 39401−39418

The pH was adjusted to 8−9. The reaction mixture was stirred under argon until TLC analysis indicated the complete disappearance of compound 7. The solvent was evaporated under a vacuum, and the crude residue was further purified by flash chromatography to give the target compound, IPTC, as an orange powder (45% yield). HRMS(ESI) m/z for C37H52N11O9:794.3949; found: 794.3963.

Several complementary assays (Figure 1) are used to evaluate the impact of IPTC on mitochondrial function. The detailed information is shown below:

2.2. PC12 Cell Survival Assay. The free radical scavenging capacity of the newly synthesized compound IPTC was evaluated in PC12 cells using Dawson's method with minor modifications.[18,28,43] In brief, PC12 cells were grown in Dulbecco's modified Eagle's medium supplemented with 10% heat-inactivated horse serum (Hyclone), 5% fetal bovine serum (GIBCO), 1.0 mM sodium pyruvate, 100 U/mL penicillin, and 100 μg/mL streptomycin at 37 °C, in 5% CO_2 atmosphere. PC12 cells were seeded in 96-well plates coated with poly-L-lysine at 20,000 cells per well during the exponential growth phase. After a 24 h attachment period, fresh media containing 12.5, 25, 50, 100, or 200 μM of tested compounds, respectively, were added to each well and were incubated for 1 h. Nitric oxide (NO) damage was then induced by adding 2 mM of sodium nitroprusside (SNP) followed by 2 h of incubation.[44] The media were replaced with fresh media, and cells were incubated for 14 h, after which cell survival was measured by a colorimetric assay with MTT according to Mosmann's method.[45] Similarly, H_2O_2 damage was induced with 1 mM H_2O_2 followed by 1 h of incubation, while hydroxy-radical ($^{\bullet}OH$) damage was caused by 1 mM H_2O_2/30 μM Fe (II) followed by 1 h of incubation.[44] Statistical analysis employed a one-way ANOVA test.

2.3. Hypoxia/Reoxygenation (H/R) Protocol. H9C2 cardiomyocytes have been routinely used as a cellular model of cardiac ischemia/reperfusion (I/R) injury in vitro.[46−50] Rat cardiomyocytes H9C2 were cultured in Dulbecco's Modified Eagle's Medium/Nutrient Mixture F-12 (DMEM/F12) supplemented with 10% (v/v) fetal bovine serum (FBS, Invitrogen Life Technologies), 100 μg/mL of penicillin and 100 μg/mL of streptomycin. Cells were cultured to 70−80% confluence for further experiments. We examined the putative protective effects of IPTC in rat cardiomyocytes H9C2 using the cellular model of hypoxia/reoxygenation (H/R), which was achieved in a flow-through chamber as previously described.[20−22] In brief, H9C2 cells were subjected to hypoxia using glucose-free and FBS-free DMEM/F12 buffer in a flow-through chamber supplied with 94% N_2, 5% CO_2, and 1% O_2 at 37 °C for 6 h. After hypoxia, the cells were transferred back to 10% FBS and DMEM/F12 under normal conditions for reoxygenation for 4 h. Normal control cells were incubated in a regular cell culture incubator under normoxic conditions.

The H9C2 cells were allocated into eight distinct groups as follows: (1) The Sham-control group, where cells were maintained under standard culture conditions; (2) The Control + Tempol group, with cells grown in the presence of Tempol (10 μM) under standard conditions; (3) The Control + Mito-Tempo group, featuring cells cultured with Mito-Tempo (10 μM) under normal conditions. It is notable that Mito-Tempo, a mitochondria-focused antioxidant, combines a piperidine nitroxide (Tempo) moiety and the lipophilic cation triphenylphosphonium (TPP+);[51−53] (4) The Control + IPTC group, where cells were cultured with IPTC (10 μM) under standard conditions; (5) The H/R group, subjected to a hypoxia/reoxygenation (H/R) protocol; (6) The H/R + Tempol group, with cells receiving a 12-h pretreatment with Tempol before the hypoxia induction and subsequent H/R protocol; (7) The H/R + Mito-Tempo group, where cells were pretreated with Mito-Tempo for 12 h before the hypoxia induction and then underwent the H/R protocol; (8) The H/R + IPTC group, involving cells pretreated with IPTC for 12 h before hypoxia induction and subsequent exposure to the H/R protocol.

2.4. Cell Viability Assay. Cell viability was evaluated with the CCK-8 kit by a microplate reader at a wavelength of 450 nm. Cell counting kit-8 (CCK-8) is a colorimetric assay for determining the number of viable cells in the cytotoxicity assay, which is more sensitive than any other tetrazolium salt such as MTT.[54] Each experiment was repeated thrice; the results are shown in Figure 2.

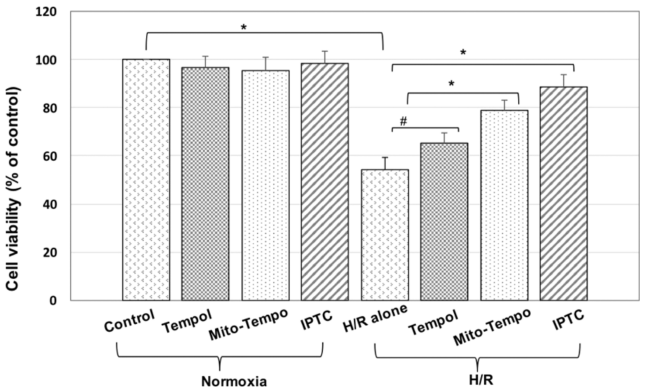

Figure 2. Effect of the tested compounds (Tempol, Mito-Tempo, and IPTC) on the cell viability of H9C2 cells subjected to H/R protocol. Data are expressed as a percentage of the sham control and are represented as mean ± SD (n = 6; #: $p < 0.05$; *: $p < 0.01$ vs H/R alone group).

2.5. Detection of Lactate Dehydrogenase (LDH). The LDH release assay is a commonly used cell cytotoxicity assay to assess plasma membrane damage in a cellular population. LDH activity was expressed as (U/L); the results are shown in Figure 3. The irreversible injury was quantitated as the percent total LDH released (values are expressed as mean ± SD; n = 6).

2.6. Detection of Malondialdehyde (MDA). An enhanced bicinchoninic acid (BCA) protein assay kit measured protein concentrations of lysis buffer. MDA is a commonly used marker for oxidative stress. For the detection of MDA, the cell lysis buffers were incubated with the reagents of the MDA assay kit, and this kit allows the quantitation of the MDA-protein adduct. MDA level was expressed as nmol/(mg protein), and the results are shown in Figure 4.

2.7. Detection of Mitochondrial ROS Generation. Cardiomyocytes H9C2 were counter-stained with MitoProbe and Hoechst 33342, respectively. MitoProbe is a group of novel fluorogenic probes specifically localized in mitochondria and can be employed both in vivo and in vitro to detect mitochondrial ROS (mtROS) generation.[57] The mtROS generation and the mitochondrial morphology changes can be directly visualized under confocal fluorescence microscopy (Figure 5A) using cell samples subjected to the same H/R protocol. The generation of mtROS and the alterations of

https://doi.org/10.1021/acsomega.4c02725
ACS Omega 2024, 9, 39401−39418

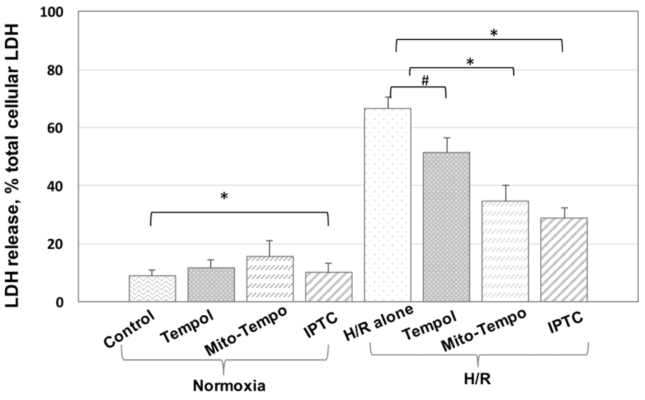

Figure 3. Effect of the tested compounds (Tempol, Mito-Tempo, and IPTC) on the lethal injury of H9C2 cells induced by H/R. Data are expressed as a percentage of total cellular LDH and are represented as mean ± SD (n = 6; #: p < 0.05; *: p < 0.01 vs H/R alone group).

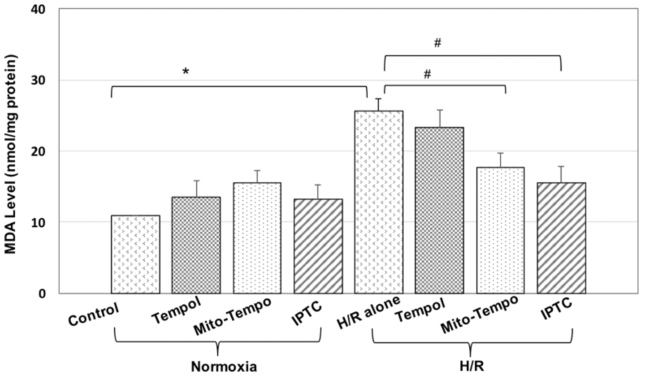

Figure 4. Effect of test compounds (Tempol, Mito-Tempol, and IPTC) pretreatment on malondialdehyde (MDA) in H9C2 cells during H/R injury. Values are expressed as mean ± SD; (n = 3; #: p < 0.05; *: p < 0.01 vs H/R alone group).

mitochondrial morphology were simultaneously examined at three different time points of H/R (i) 0 h before cells were subjected to H/R; (ii) immediately after 6 h of hypoxia; (iii) immediately after 6 h of hypoxia followed by 4 h of reoxygenation. Before quantifying the alterations of the mean fluorescence intensity (MFI) of MitoProbe, the confocal fluorescence images were preprocessed (Figure 5B) to improve the quality of binarized images. By measuring the MFI of MitoProbe changes in the binarized images, the total ROS generation in the mitochondria was quantitatively determined, and the results are shown in Figure 5C. Error bars indicate the mean (SEM) standard error from at least four independent experiments. (#: compared with control at baseline, p < 0.01; *: compared with H/R alone, p < 0.01).

2.8. Mitochondrial Morphology Analysis. Cells were counter-stained with MitoTracker (green fluorescence) for mitochondrial morphological analysis. The mitochondrial morphology was classified into three categories: tubular (normal), intermediate (tubular with swollen regions), and fragmented (small and globular) (Figure 5D). The method for quantification involved determining the percentage of cells with abnormal mitochondrial morphologies as a surrogate for the proportion of cells with fragmented mitochondria. When cells with intermediate or fragmented mitochondria were expressed as a percentage of the total cells counted (100 cells were counted per experiment, and the data was averaged over four independent experiments per treatment), the nontreated cells contained predominantly long and evenly distributed tubular mitochondria throughout the cell. Error bars indicate SEM from at least four independent experiments (#: compared with H/R alone, p < 0.05; *: compared with H/R alone, p < 0.01). The results are presented in Figure 5E.

2.9. Detection of Mitophagy. Microscopy-based green fluorescent protein GFP-LC3 puncta formation assay is commonly used for measuring autophagic activity.[22] To further examine the effect of **IPTC** on the degradation of mitochondria by autophagy (mitophagy), H9C2 cells were transfected with GFP-LC3. Then, the GFP-LC3 transfected H9C2 cells were costained with MitoProbe.[44] Rapamycin is a known inducer of autophagy.[22,55] Rapamycin was used as a positive control in our present study. Ten fields of view were randomly selected for each sample, and the percentages of cells with GFP-LC3 positive punctate, MitoProbe positive, and their colocalization (dual-positive, GFP-LC3+/MitoProbe+) were calculated, respectively. The results are shown in Figure 6.

In this assay, H9C2 cells were divided into five groups: (1) Sham-control group, cells were cultured under normal conditions; (2) Hypoxia (H) group, cells were subjected to 6h of hypoxia (H); (3) H/R group, cells were subjected to hypoxia/reoxygenation protocol (H/R); (4) H/R + rapamycin (10 μM) group, cells pretreated with rapamycin for 12 h before induction of hypoxia and then subjected to H/R protocol; (5) H/R + **IPTC** (10 μM) group, cells pretreated with **IPTC** for 12 h before induction of hypoxia and then subjected to H/R protocol.

2.10. Detection of mPTP Opening. In this assay, H9C2 cells were divided into nine groups: (1) Sham-control group; (2) Control + rapamycin (10 μM) group; cells were cultured with rapamycin (10 μM) under normal conditions. (3) Control + IPTC (10 μM) groups; cells were cultured with IPTC (10 μM) under normal conditions. (4) Hypoxia (H) group, cells were subjected to 6h of hypoxia (H); (5) Hypoxia + rapamycin (10 μM) group, cells pretreated with rapamycin for 12 h before induction of hypoxia and then subjected to 6h of hypoxia; (6) Hypoxia + IPTC (10 μM) group, cells pretreated with IPTC for 12 h before induction of hypoxia and then subjected to 6h of hypoxia; (7) H/R group, cells were subjected to hypoxia/reoxygenation protocol (H/R); (8) H/R + rapamycin (10 μM) group, cells pretreated with rapamycin for 12 h before induction of hypoxia and then subjected to H/R protocol; (9) H/R + IPTC (10 μM) group, cells pretreated with IPTC for 12 h before induction of hypoxia and then subjected to H/R protocol.

Briefly, rat cardiomyocytes H9C2 were incubated with calcein (fluorescein complex; 2 μM) and $CoCl_2$ (1 mM) in Hank's Balanced Salt Solution (HBSS)/Ca^{2+} at 37 °C for 15 min. Calcein can passively diffuse into cells. Calcein-AM is a membrane-permeable fluorophore. It can quickly diffuse into all subcellular compartments, including mitochondria.[56] Ubiquitous intracellular esterase can readily cleave the fluorophore's acetoxymethyl (AM) group. Because of its hydrophilicity, calcein is then trapped within all subcellular compartments. Thus, calcein can accumulate in the cytosol and mitochondria, and its corresponding fluorescence can be observed. The cells are then loaded with the divalent cobalt cation (Co^{2+}). $CoCl_2$ can quench the cytosolic fluorescence, whereas the fluorescence from the mitochondria can be maintained because of the intact inner mitochondrial membrane.[56] The opening of the mPTP enables cobalt to

https://doi.org/10.1021/acsomega.4c02725
ACS Omega 2024, 9, 39401−39418

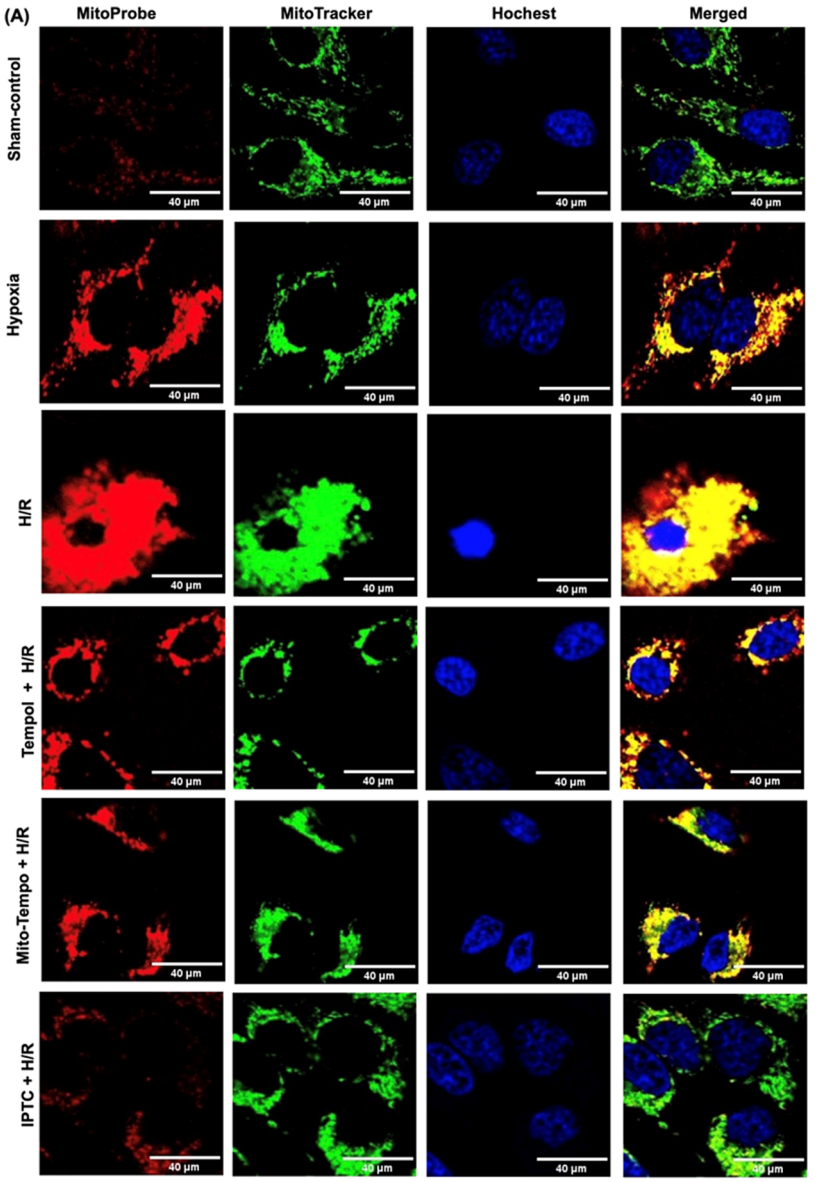

Figure 5. continued

https://doi.org/10.1021/acsomega.4c02725
ACS Omega 2024, 9, 39401−39418

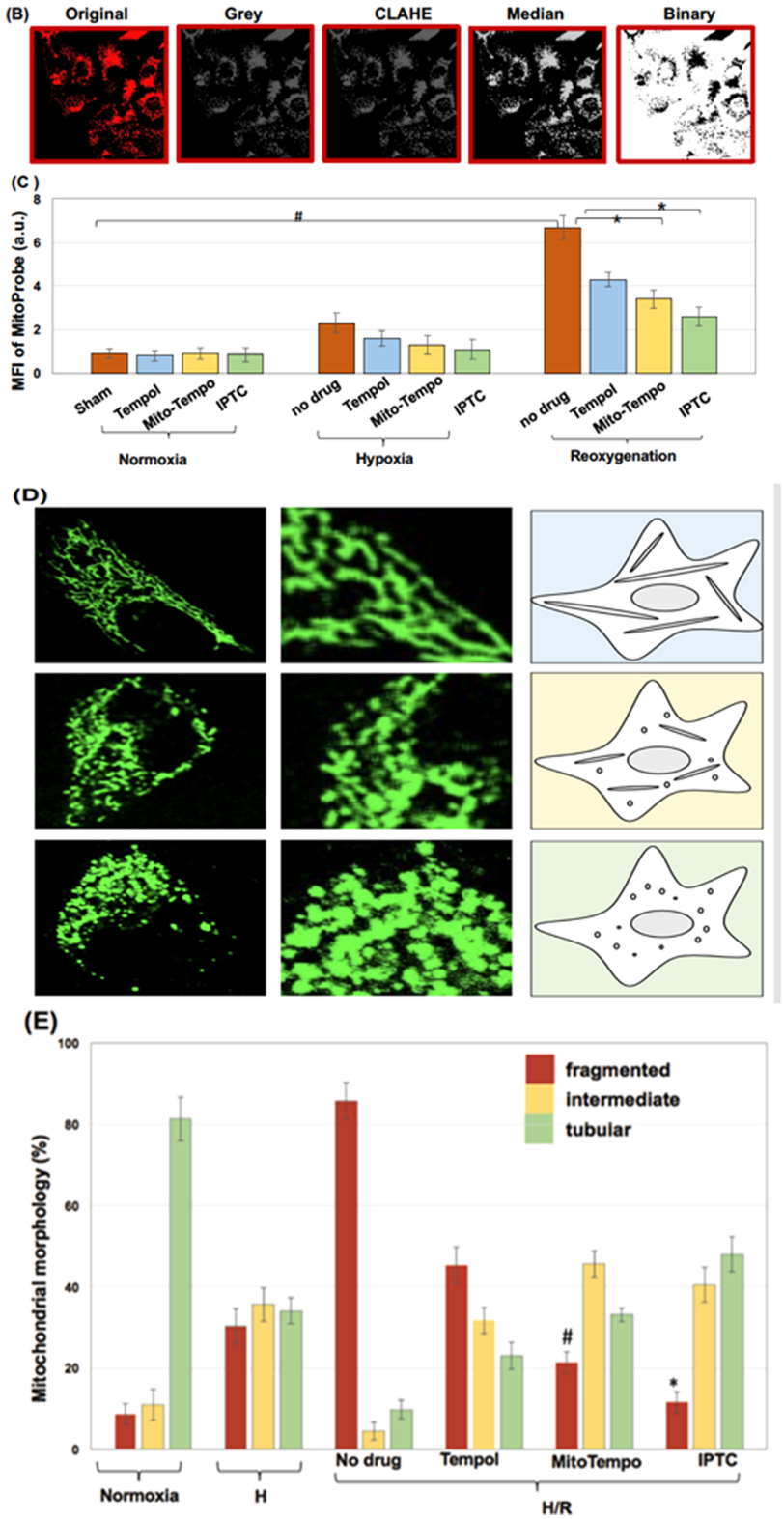

Figure 5. IPTC inhibited mitochondrial ROS production and mitochondrial fragmentation in H9C2 cells subjected to H/R protocol: (A) Representative confocal microscopic images of H9C2 rat cardiomyocytes counter-stained with MitoProbe (100 nM, red fluorescence), MitoTracker (green fluorescence) and Hoechst 33342 (blue fluorescence): Fluorescent images are displayed for cells from a sham-control group (no H/R), cells subjected to hypoxia or cells subjected to H/R with/without drug (Tempol, MitoTempo, and IPTC) treatment; (B) The confocal fluorescence images were preprocessed to improve the quality of binarized images. (C) The total ROS generation in the mitochondria was quantified by measuring the mean fluorescence intensity (MFI) of MitoProbe changes in the binarized images. (D) Mitochondrial morphology was categorized as follows: tubular, intermediate, and fragmented. (E) Mitochondrial morphology analysis of H9C2 cells subjected to H/R with/without the drug (Tempol/Mito-Tempo/IPTC) treatment. Cells were imaged on an inverted laser scanning fluorescent microscope (Olympus) using a 60 x oil immersion objective lens.

https://doi.org/10.1021/acsomega.4c02725
ACS Omega 2024, 9, 39401−39418

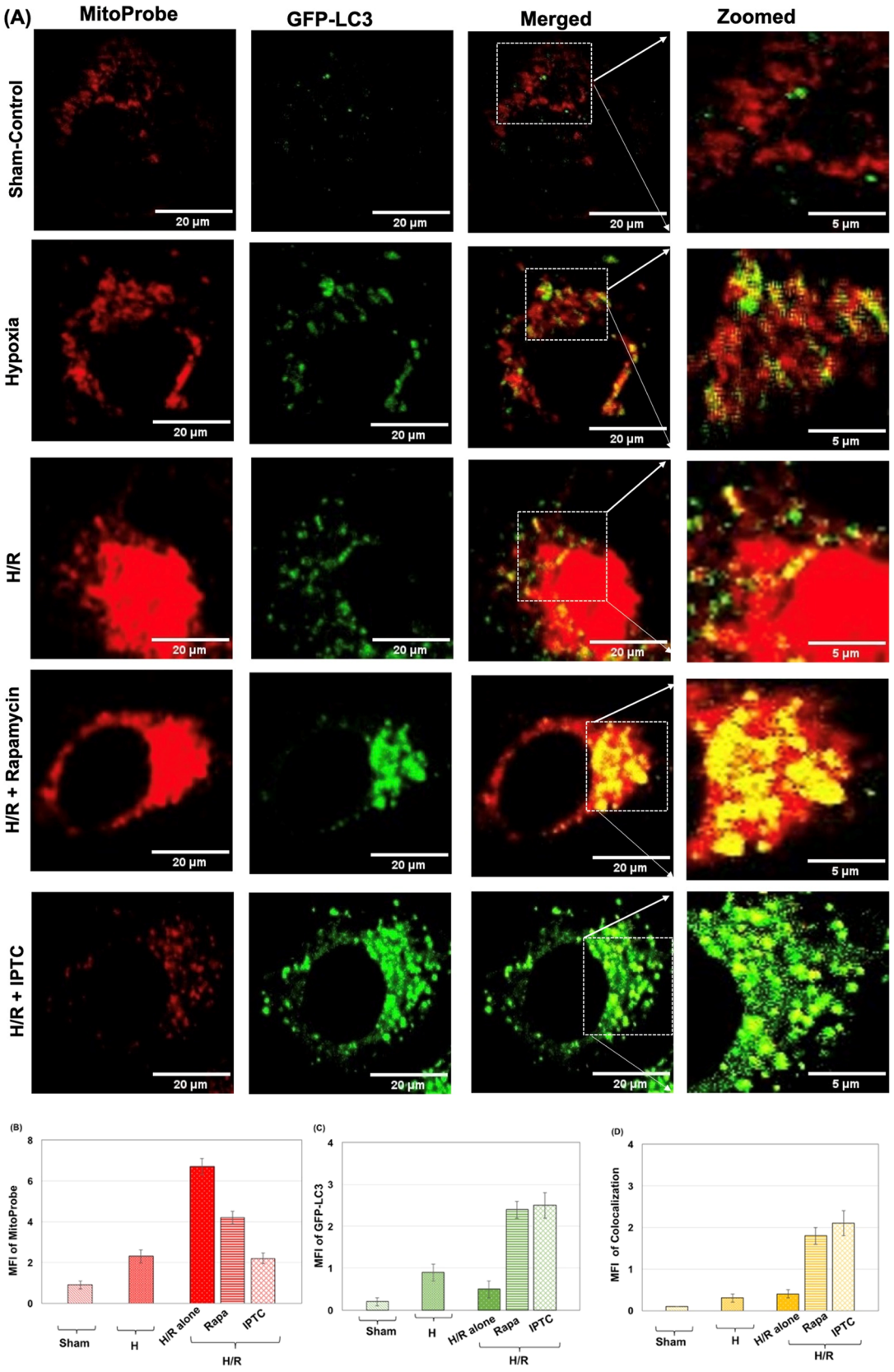

Figure 6. IPTC enhances mitophagy in H9C2 rat cardiomyocytes subjected to H/R. (A) Representative confocal fluorescent images of rat cardiomyocytes H9C2 subjected to different treatment protocols during H/R. (B) mitochondrial ROS level was determined by measuring the mean fluorescence intensity (MFI) of MitoProbe; (C) autophagosome formation was estimated by measuring the MFI of changes; and (D) the colocalization index, gauging mitophagy activity, was produced by calculating the MFI of double-positive (GFP-LC3+/ MitoProbe+) cells with yellow fluorescence. Cells were imaged on an inverted laser scanning fluorescent microscope (Olympus) using a 60× oil immersion objective lens.

https://doi.org/10.1021/acsomega.4c02725
ACS Omega 2024, 9, 39401−39418

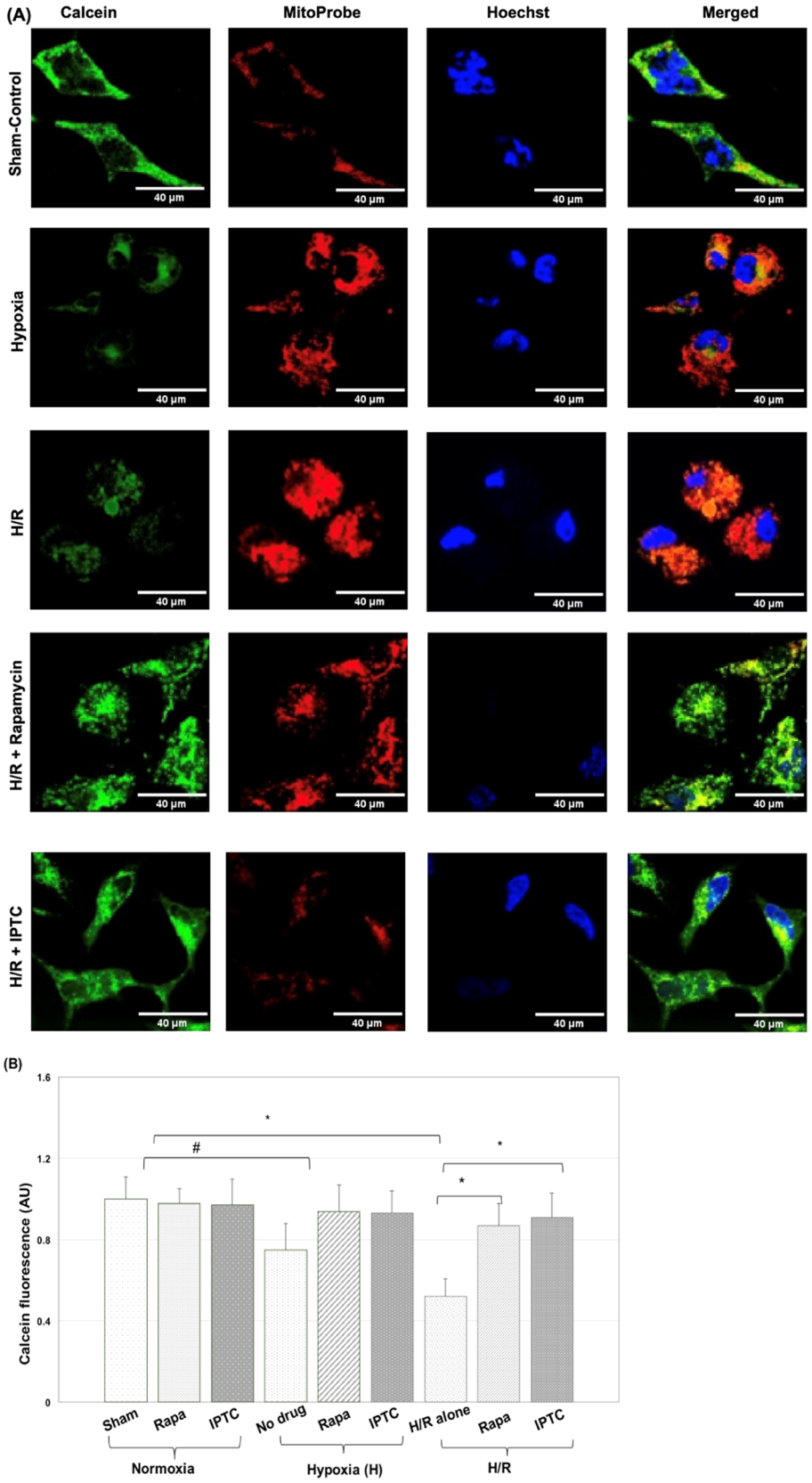

Figure 7. IPTC inhibits mPTP opening during hypoxia/reoxygenation (H/R). (A) Representative confocal microscopic images of H9C2 rat cardiomyocytes after incubation with calcein-AM (1 μM, green fluorescence), Co^{2+} (1 mM), and MitoProbe (1 μM, red fluorescence), and Hoechst 33342 (blue fluorescence): Fluorescent images are displayed for cells from a sham-control group (no H/R), cells subjected to hypoxia (H), or cells subjected to H/R with/without rapamycin/IPTC treatment; Cell were imaged on an inverted laser scanning fluorescent microscope (Olympus) using a 60 x oil immersion objective lens. (B) Quantifying mitochondrial calcein fluorescence in H9C2 cardiomyocytes subjected to H/R in the absence/presence of rapamycin/IPTC.

https://doi.org/10.1021/acsomega.4c02725
ACS Omega 2024, 9, 39401−39418

Scheme 1. Synthetic Route for IPTC[a]

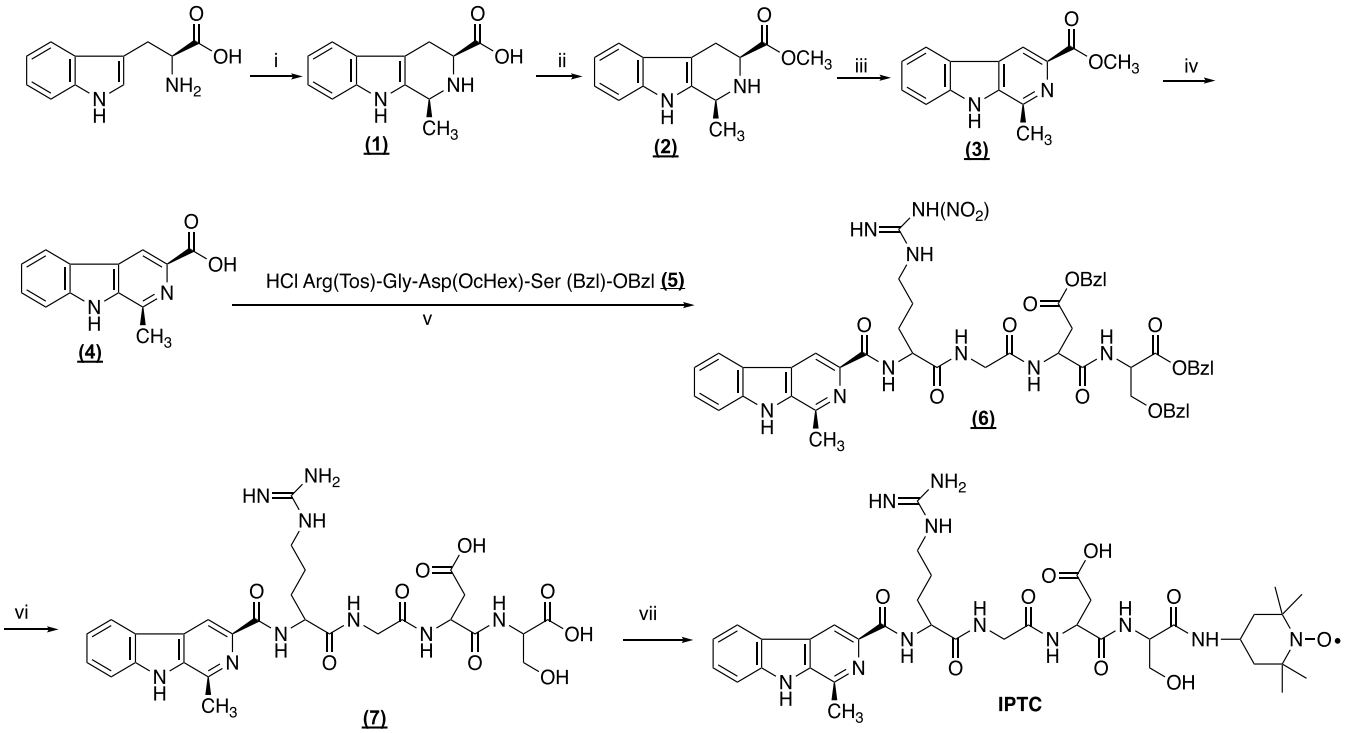

[a]Reagents: (i) H_2SO_4, CH_3CHO; (ii) $SOCl_2$; (iii) sulfur; (iv) NaOH(aq); (v) compound **5**, *N*,*N*′-dicyclohexylcarbodiimide (DCC); (vi) hydrogen fluoride (HF); (vii) 4-amino-Tempo, DCC.

enter mitochondria, resulting in the quenching of calcein fluorescence in the mitochondria. Before quantifying the alterations of the MFI of the calcein fluorescence, the confocal fluorescence images were preprocessed to improve the quality of binarized images. Error bars indicate the mean SEM from at least four independent experiments. The results are shown in Figure 7.

3. RESULTS

3.1. Synthesis of IPTC. Starting from the optically active L-tryptophan, following esterification of the carboxylic moiety with MeOH/$SOCl_2$, the resulting L-tryptophan methyl ester was then subjected to Pictet−Spengler cyclization with acetaldehyde to yield 1-methyl-1,2,3,4-tetrahydro-β-carboline-3-carboxylate **2** in 45% yield. The conversion of the 1,2,3,4-tetrahydro-β-carboline derivative **2** to the corresponding β-carboline derivative **3** (67% yield) was carried out via oxidation of the tetrahydro-β-carboline derivatives with sulfur in refluxing xylene. Subsequently, compound **3** was hydrolyzed in the presence of sodium hydroxide to provide the critical intermediate **4** (83% yield). The protected tetrapeptide intermediates were prepared according to the synthetic route in Scheme 1. The protected tetrapeptide intermediate **5** was prepared via the solution method. The conjugation of **4** and the protected tetrapeptide fragment **5** subsequently proceeded smoothly to give compound **6**. After removing the protective groups, compound **7** was subjected to conjugation with 4-amino Tempo, and the desired product IPTC was obtained with a moderate yield (45% yield).

3.2. In Vitro Antioxidant and Free Radical Scavenging Activity of IPTC Evaluated in PC 12 Cell Lines. Rat pheochromocytoma (PC12) cells originating from the adrenal medulla, synthesizing and releasing catecholamines. PC12 cells are susceptible to oxidative stress, and it has been extensively used for in vitro ischemia studies.[23,24,26] Herein, the free radical scavenging properties of **IPTC** against $^{\bullet}NO$, $^{\bullet}OH$, and H_2O_2 were evaluated using PC12 cell survival assay and compared with that of Tempol. The results were expressed as EC_{50} (μM) values. The reduction of viability induced by exposure to free radicals was curtailed with the incubation of the tested compounds.

In this study, IPTC significantly outperformed Tempol and its precursor in scavenging hydroxyl radicals, evidenced by its lower EC_{50} value (15.7 ± 2.5 μM, $p < 0.001$). It also offered better protection against hydrogen peroxide, with an EC_{50} of 31.3 ± 3.4 μM ($p < 0.01$). Additionally, IPTC was equally or more effective against nitric oxide when compared to both reference compounds (Table 1). These findings suggest

Table 1. Free Radical Scavenging Activity of Tested Compounds in PC12 Cell Survival Assay

	EC_{50} (μM) (X ± SD)		
compound	$EC_{50}/^{\bullet}NO$	EC_{50}/H_2O_2	$EC_{50}/^{\bullet}OH$
Tempol	90.4 ± 4.5	65.7 ± 2.8	84.3 ± 3.2
compound **4**	88.7 ± 4.6	56.4 ± 4.3	91.0 ± 4.7
IPTC	61.5 ± 3.7	31.3 ± 3.4[a]	15.7 ± 2.5[b]

[a]$p < 0.01$. [b]$p < 0.001$.

IPTC's potential as a potent antioxidant for therapeutic use in oxidative stress-related conditions, displaying greater potency in neutralizing specific free radicals affecting PC12 cells.

3.3. IPTC's Role in Enhancing Cell Viability and Reducing Cellular Damage in Hypoxia/Reoxygenation (H/R) Conditions. This research used H9C2 cells analogous

https://doi.org/10.1021/acsomega.4c02725
ACS Omega 2024, 9, 39401−39418

to cardiomyocytes to create an in vitro I/R injury model. The model effectively replicated hypoxia followed by reoxygenation, a crucial aspect for analyzing cellular behavior under controlled settings. Using the CCK-8 assay, we observed a notable decrease in cell viability under H/R conditions compared to normal oxygen levels. This finding confirmed the model's reliability in simulating ischemic conditions. We also explored the protective effects of several compounds, including Tempol, Mito-Tempo, and, notably, IPTC. Mito-Tempo and IPTC markedly improved cell viability following H/R stress, pointing to their potential as treatments for cardiac ischemic conditions like myocardial infarction. Their consistent cytoprotective effect in this study underscores their therapeutic promise.

In addition to viability, the study assessed cellular damage in H/R stress by measuring lactate dehydrogenase (LDH) and malondialdehyde (MDA) levels. LDH, typically contained within healthy cells, is released following cellular damage, and its increased levels during H/R indicated enhanced cell damage. Pretreatment with Tempol, Mito-Tempo, and especially IPTC significantly lowered LDH release, suggesting their effectiveness in protecting against cell membrane damage. Similarly, MDA levels, which signal lipid peroxidation and oxidative stress, rose after H/R. However, treatment with Mito-Tempo or IPTC substantially reduced MDA levels, emphasizing their antioxidant capabilities and role in reducing oxidative damage. These results indicate that Mito-Tempo and IPTC effectively minimize cell membrane damage and oxidative stress in H9C2 cells under H/R conditions. This efficacy presents them as promising therapeutic agents for managing cardiac tissue damage in myocardial ischemia/reperfusion injury, typical in heart attacks and similar cardiac incidents. The pronounced decrease in LDH and MDA levels following these treatments highlights their potential to reduce cell death and tissue damage in critical conditions.

3.4. IPTC Inhibited Mitochondrial Fragmentation and Mitochondria-Derived ROS (mtROS) Production in H9C2 Cells Subjected to H/R Protocol. During hypoxia, specific cells exhibited an increased mean fluorescence intensity (MFI) of MitoProbe signals within the mitochondrial network surrounding the nucleus (row 2, Figure 5A). On the other hand, during reoxygenation, the mitochondrial network became dispersed and irregular with an enhanced MFI of MitoProbe. The MFI of MitoProbe signals increased significantly during H/R compared to baseline values. However, pretreatment with either Mito-Tempo or IPTC significantly reduced the increase in the MFI of MitoProbe signals during H/R. The total generation of reactive oxygen species (ROS) in the mitochondria was determined by monitoring the changes in the MFI of MitoProbe signals at different time points of H/R. Our current studies indicate an approximately 2.5-fold increase in mtROS during the hypoxia phase (row 2, Figure 5A; see Figure 5C for quantitative values). Furthermore, 6 h of hypoxia followed by 4 h of reoxygenation resulted in an approximately 7.4-fold rise in mtROS (row 3, Figure 5A; see Figure 5C for quantitative values). Cells pretreated with either Mito-Tempo or IPTC showed significantly lower mtROS levels, suggesting that the elevated mtROS generation induced by H/R could be significantly mitigated by Mito-Tempo (row 5, Figure 5A; see Figure 4C for quantitative values) or IPTC intervention (row 6, Figure 5A; see Figure 5C for quantitative values).

In this study, we also examined the effect of IPTC on mitochondrial morphology. In normal, sham control cells, mitochondria appear as long tubular structures with low MFI of MitoProbe (row 1, Figure 5D). During hypoxia, there was a significant increase in the number of cells with intermediate and fragmented mitochondria (row 2, Figure 5D), with a corresponding decrease in the percentage of cells with long tubular mitochondria. Reoxygenation resulted in most cells displaying fragmented mitochondria with shorter and spherical structures (row 3, Figure 5D). The percentage of cells exhibiting long tubular mitochondria decreased significantly from 81.3 ± 5.4% in sham control cells to 9.8 ± 2.3% in cells exposed to H/R alone.

In contrast, mitochondria with intermediate and fragmented morphology were predominantly aggregated in the perinuclear region (row 3, Figure 5A). However, adding Mito-Tempo or IPTC to the control cell perfusate undergoing hypoxia significantly protected against H/R-induced cell death and attenuated the fragmented mitochondrial appearance. Cells treated with IPTC + H/R showed a significant decrease in the percentage of cells with fragmented mitochondria compared to cells exposed to H/R alone (IPTC + H/R: 85.7 ± 4.5% vs H/R alone: 11.5 ± 2.6%) (row 6, Figure 5A; see Figure 5E for quantitative values).

3.5. IPTC Induces Protective Mitophagy against H/R Injury. The study aimed to investigate the role of IPTC in inducing protective mitophagy against H/R injury. To monitor the mitophagy response during H/R, H9C2 cells were transfected with GFP-LC3 to label autophagosomal membranes. The punctate formation of GFP-LC3 was used for quantitative analysis of autophagosomes. To study the relationship between mitophagy and mtROS production, GFP-LC3 transfected H9C2 cells were labeled with MitoProbe for real-time monitoring of GFP-LC3 labeling and MitoProbe colocalization. The colocalization of the oxidatively "stressed" mitochondria (visualized by MitoProbe,[25,44] red fluorescence) with autophagosomes (visualized by GFP-LC3,[22,55] green fluorescence) showed the successful fusion between damaged mitochondria with autophagosomes for trafficking to lysosomes for degradation.

Compared to the sham control groups (row 1, Figure 6A), the percentage of cells with GFP-LC3 punctate increased during the hypoxia phase (row 2, Figure 6A). In contrast, the rate of cells with GFP-LC3 punctate remained unchanged during reoxygenation. Most mitochondria became fragmented, accompanied by significantly increased mtROS after reoxygenation (row 3, Figure 6A). However, treating H9C2 cells with IPTC significantly increased the number of autophagosomes (visualized by GFP-LC3, green fluorescence) (row 5, Figure 6A; see Figure 6C for quantitative values) and reduced the elevated mtROS levels induced by H/R (row 5, Figure 6A; see Figure 6B for quantitative values). After IPTC treatment, most of the oxidatively "stressed" mitochondria (visualized by MitoProbe, red fluorescence) were found to be colocalized with autophagosomes (pictured by GFP-LC3, green fluorescence), resulting in damaged mitochondria being incorporated into autolysosomes (visualized by double-positive MitoProbe+/GFP-LC3+, yellow fluorescence). This suggests that the dysfunctional mitochondria were selectively delivered for autophagic degradation (mitophagy). IPTC-pretreated cells showed a level of mitophagy activity comparable to rapamycin-treated cells (row 4, Figure 6A).

https://doi.org/10.1021/acsomega.4c02725
ACS Omega 2024, 9, 39401−39418

3.6. IPTC Inhibits mPTP Opening during Hypoxia/Reoxygenation (H/R). In this experiment, we evaluated the opening of mitochondrial permeability transition pores (mPTP) in H9C2 rat cardiomyoblasts. We used the calcein-AM assay (calcein-AM, AM = acetoxymethyl) to perform this evaluation.[56] During hypoxia (row 2, Figure 7), we observed calcein fluorescence solely within the mitochondrial matrix, as the inner mitochondrial membrane does not allow the passage of Co^{2+}. However, during the late stage of reoxygenation (row 3, Figure 7), we noticed that the mitochondrial calcein fluorescence was quenched due to the opening of the mPTP. In contrast, the mitochondrial calcein fluorescence was considerably higher in cells treated with rapamycin + H/R (row 4, Figure 7) or IPTC + H/R (row 5, Figure 7) than in cells treated with H/R alone. This suggests that rapamycin or IPTC pretreatment could effectively inhibit the opening of mPTP.

4. DISCUSSION

As a first step, we explored the antioxidant and free radical scavenging abilities of IPTC, utilizing PC 12 cell lines derived from rat pheochromocytoma. These cells, susceptible to oxidative stress due to their ability to produce catecholamines, offer an accurate in vitro model for mimicking ischemic conditions.[18,23,28,30,31] We assessed IPTC's effectiveness at neutralizing crucial free radicals, including nitrogen oxide ($^{\bullet}NO$), hydroxyl ($^{\bullet}OH$) radicals, and hydrogen peroxide (H_2O_2), through cell survival assays. This assessment was benchmarked against Tempol, a recognized antioxidant, with the effectiveness measured in EC_{50} values—the concentration necessary to achieve half of the maximum effect. Our results indicated a significant finding: IPTC not only outperformed Tempol and its precursor in scavenging hydroxyl radicals, as shown by a notably lower EC_{50} value of 15.7 ± 2.5 μM, but also provided enhanced protection against hydrogen peroxide, with an EC_{50} of 31.3 ± 3.4 μM. Equally important was IPTC's comparable or superior efficacy in nitric oxide scavenging relative to the reference compounds. This aspect of IPTC's activity is especially relevant for treating I/R injury, as it hints at IPTC's ability to moderate nitric oxide levels. Doing so, IPTC may reduce excessive inflammation and promote vasodilation, which is crucial for improving blood flow and reducing damage upon reperfusion.

While the scavenging of $^{\bullet}NO$ by IPTC may raise concerns due to the generally beneficial role of $^{\bullet}NO$ in vascular health, it is crucial to understand the context in which this activity becomes advantageous, especially in the setting of I/R injury. Our findings reveal that IPTC surpasses Tempol in neutralizing hydroxyl radicals and effectively shields against hydrogen peroxide toxicity. Notably, the ability of IPTC to scavenge nitric oxide surpasses that of reference compounds, a property that plays a pivotal role in the context of I/R injury.

The benefit of IPTC's nitric oxide scavenging emerges from its potential to fine-tune $^{\bullet}NO$ levels within the ischemic tissue. In the delicate environment of I/R injury, excessive nitric oxide production can lead to detrimental nitrosative stress, exacerbating tissue damage by forming peroxynitrite and other reactive nitrogen species. By moderating $^{\bullet}NO$ levels, IPTC helps mitigate these harmful effects, reducing excessive inflammation that can further impair tissue recovery. Furthermore, by controlling $^{\bullet}NO$ levels, IPTC supports the maintenance of appropriate vasodilation responses, essential for restoring blood flow and promoting the delivery of oxygen and nutrients during the reperfusion phase. Thus, the nuanced regulation of nitric oxide by IPTC contributes to a balanced recovery process, making it a promising approach for minimizing the damage and enhancing tissue repair following I/R injury.

The significant antioxidant and free radical scavenging activities of IPTC bear profound implications for I/R injury treatment. Oxidative stress is a critical factor that aggravates tissue damage in the reperfusion phase of I/R injury, where the reintroduction of oxygen leads to increased production of harmful free radicals. IPTC's capacity to efficiently neutralize these radicals indicates its significant potential to alleviate significantly the oxidative damage associated with I/R injury. This suggests that IPTC could be a valuable therapeutic option to promote tissue recovery and protect against the oxidative stress typically observed in such conditions, with its nitric oxide scavenging ability enhancing its therapeutic profile by potentially improving vascular responses and reducing inflammation during reperfusion.

Our data highlights the promise of IPTC in treating I/R injury, showcasing several properties that underline its potential therapeutic value. IPTC has significantly boosted cell viability in H9C2 cells, analogous to cardiomyocytes, under stress from H/R. This enhancement suggests IPTC's capability to protect heart cells during heart attacks, where the blood supply is interrupted and restored. Additionally, IPTC's impact extends to cellular integrity, as evidenced by its ability to reduce LDH release. Lower levels of LDH indicate minimized cell membrane damage, a critical benefit during ischemia-reperfusion episodes.

Complementing its effects on cell viability and structural preservation, IPTC also exerts antioxidative action. This is illustrated by the observed reduction in MDA levels following IPTC treatment. MDA, a marker of oxidative stress due to lipid peroxidation, signals cell damage in high concentrations. The ability of IPTC to decrease MDA levels points to its role in mitigating oxidative stress, a key player in the pathogenesis of ischemia-reperfusion injury. With such properties, IPTC emerges as a potential therapeutic agent capable of diminishing the detrimental effects often seen postreperfusion, particularly in the cardiac tissue affected by myocardial infarction.

The collective data on IPTC reinforce its profile as a cytoprotective agent with considerable promise. It offers a dual shield against the initial ischemic insult and the subsequent reperfusion injury by preserving cell viability, curtailing cellular injury, and combating oxidative stress. Such multifaceted protection by IPTC could be instrumental in preventing the sequence of cellular events that escalate into extensive cell death and tissue damage. Hence, IPTC's comprehensive therapeutic effects could significantly limit cardiac muscle damage during ischemia-reperfusion events, critical moments where timely and effective treatment is crucial.

Our further investigation reveals that IPTC may offer protective effects against I/R injury through various mechanisms. One significant aspect is the mitigation of mitochondrial fragmentation. As the cellular powerhouses, mitochondria's functionality is closely tied to their structural integrity. Under the duress of hypoxia and subsequent reoxygenation, a typical reaction of mitochondria is to fragment, correlating with cell harm and death. IPTC appears to safeguard mitochondrial structure, evidenced by a reduction in fragmentation in pretreated cells, implying that IPTC is vital in maintaining

https://doi.org/10.1021/acsomega.4c02725
ACS Omega 2024, 9, 39401−39418

mitochondrial integrity during I/R injury, which is paramount for cellular survival and performance.

Additionally, our data points to a noteworthy reduction in the production of mtROS following IPTC treatment. Elevated mtROS levels during I/R injury contribute significantly to cellular damage. The observed decrease in mtROS with IPTC suggests a potential antioxidative role, which could curtail oxidative stress and subsequent cell damage, thus preserving mitochondrial functionality and preventing cell death pathways from activating.

Furthermore, preserving the mitochondrial network is another critical action of IPTC. Maintaining a continuous mitochondrial network is essential for energy distribution throughout the cell, and the dispersal and irregularity induced by reoxygenation are typically detrimental. Our findings suggest that IPTC supports the maintenance of this network, ensuring efficient cellular respiration and energy production necessary for cell vitality.

IPTC's influence extends to cytoprotection, as demonstrated by the substantial reduction in cells exhibiting mitochondrial fragmentation after IPTC treatment compared to those subjected to H/R alone. This cytoprotective role could be pivotal in shielding cells from the deadly consequences of I/R injury. With its multifaceted ability to maintain mitochondrial structure and function amidst the stresses of hypoxia and reoxygenation and by reducing oxidative stress, IPTC emerges as a promising therapeutic candidate for mitigating the cellular destruction typical of I/R injury, a key concern in conditions like myocardial infarction. This positions IPTC as a potentially valuable agent in treating I/R injury, especially considering the heart's reliance on mitochondrial energy production.

Mitophagy, a selective process crucial for maintaining mitochondrial health and cellular integrity, is essential during I/R injury, where cellular structures undergo considerable stress. Our research illuminates the pivotal role of IPTC in fostering protective mitophagy in H9C2 cells subjected to I/R injury, thus underscoring its therapeutic promise. IPTC's capacity to instigate mitophagy emerges as a linchpin in cellular responses to such insults, affirming its therapeutic significance.

During ischemia, especially reperfusion, damaged mitochondria escalate mtROS production, precipitating a harmful cycle of mitochondrial deterioration and cellular demise. IPTC intercedes by fostering the elimination of these compromised mitochondria, thus curbing mtROS generation and attenuating cellular damage, thereby priming the groundwork for recuperation.

Removing dysfunctional mitochondria via IPTC-induced mitophagy assumes particular salience during reperfusion, a phase marked by heightened ATP demand. Efficient mitophagy ensures the preservation of a pool of robust, functional mitochondria capable of meeting this augmented energy requirement. Upholding this energetic equilibrium emerges as indispensable for cell survival and post-I/R injury recovery, forestalling catastrophic cellular malfunction.

Moreover, IPTC's efficacy in promoting mitophagy is underscored by its comparable performance to rapamycin, a recognized autophagy enhancer.[22,55] This comparison intimates that IPTC could furnish a similarly efficacious alternative for inducing mitophagy, enriching the therapeutic armamentarium. Such a mechanism is essential in forestalling the release of pro-apoptotic factors from damaged mitochondria, thereby averting the apoptotic cascade and programmed cell demise.

The opening of the mitochondrial permeability transition pore (mPTP) plays a crucial role in the progression of I/R injury. It triggers the collapse of the mitochondrial membrane potential, interrupts ATP synthesis, releases pro-apoptotic factors, and ultimately leads to cell death. Thus, therapeutic approaches targeting mPTP opening can significantly mitigate I/R injury.[54,57−60]

In the experiment, the calcein-AM assay was employed to assess mPTP activity. This assay relies on monitoring the retention of calcein fluorescence within mitochondria. Under hypoxic conditions, the inner mitochondrial membrane prevents cobalt (Co^{2+}) from entering, allowing calcein to remain fluorescent within the mitochondrial matrix, indicating closed mPTPs. However, mPTP opening occurs during reoxygenation, reducing mitochondrial calcein fluorescence as cobalt enters the mitochondria and binds to calcein.[56]

In the context of IPTC treatment, the sustained high levels of mitochondrial calcein fluorescence indicate that IPTC effectively inhibits mPTP opening during the reoxygenation phase of I/R injury. By preventing mPTP opening, IPTC maintains mitochondrial membrane potential, sustains ATP synthesis, and prevents the release of pro-apoptotic factors. This inhibition is crucial for preserving cardiomyocyte viability during the reperfusion phase, where significant damage often occurs due to the sudden influx of ions and restoration of blood flow, overwhelming the cells.

The therapeutic implications of IPTC's ability to inhibit mPTP opening during I/R injury are profound. By safeguarding mitochondria's structural and functional integrity, IPTC can mitigate cell death pathways, enhancing the likelihood of cell survival after an ischemic event such as myocardial infarction. Consequently, IPTC can diminish heart muscle damage, improve recovery outcomes, and reduce the risk of subsequent cardiac dysfunction. Comparing IPTC to rapamycin, another mPTP inhibitor, further underscores its potential as an effective therapeutic agent in cardiac I/R injury.

The proposed mechanism of action for IPTC revolves around its distinctive dual role as both an antioxidant and a promoter of mitophagy, presenting a novel strategy for cardioprotection. IPTC's interaction with cells occurs in various chemical forms dictated by the cellular redox environment. In hypoxic stress conditions, such as in inflammatory cells, IPTC rapidly converts to its hydroxylamine form, while in oxygen-rich cells like cardiomyocytes, it maintains its nitroxide form. This reversible redox chemistry enables IPTC to continuously modulate the balance of reduction and oxidation within the cell, which is crucial for repairing mitochondrial damage and initiating the removal of severely impaired mitochondria through mitophagy.

The mechanism of action of IPTC is multifaceted: it is postulated to adaptively regulate mitophagy in response to varying levels of mitochondrial oxidative stress, thus maintaining mitochondrial homeostasis. Additionally, the RGD motif in IPTC prevents cellular aggregation. At the same time, its nitroxide group functions akin to superoxide dismutase (SOD), aiding in the quenching of superoxide radicals and further enhancing the cytoprotective effects of IPTC.

Our comprehensive studies (Figure 1) underscore the pivotal role of mitophagy in ensuring mitochondrial quality control, suggesting that its pharmacological modulation could be transformative in protecting heart tissue. We advocate for a

https://doi.org/10.1021/acsomega.4c02725
ACS Omega 2024, 9, 39401−39418

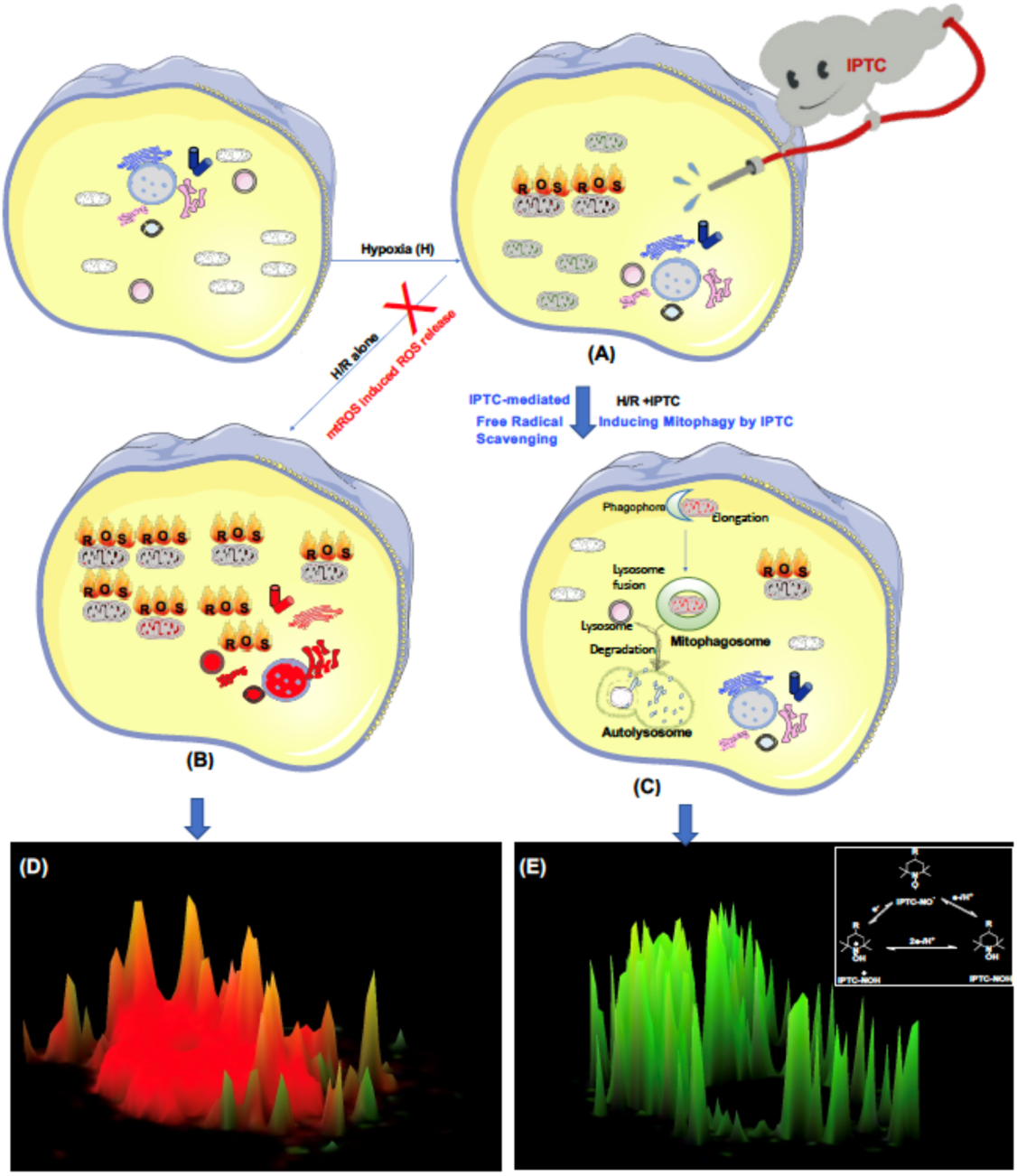

Figure 8. IPTC can put out a "fire" in the heart's mitochondria. The initial mtROS generated during hypoxia (A) can induce neighboring mitochondria to release more ROS (B), the so-called "ROS triggered ROS to release." Thus, extensive mitochondrial damage overwhelms autophagosomes and their capacity to remove damaged mitochondria. During H/R, nitroxide metabolism constantly occurs by reducing the nitroxide form (IPTC-NO$^{\bullet}$) to hydroxylamine (IPTC-NOH). IPTC-NO$^{\bullet}$, having a single unpaired electron, can continuously undergo redox transformations between the one-electron oxidized state, the oxoammonium cation $\left(\text{IPTC-N}\overset{\oplus}{\text{O}}\right)$, and the one-electron reduced IPTC-NOH. Under the balanced redox microenvironment (C), the mitochondria undergo constant damage repair through mitochondrial dynamics, whereas severely damaged mitochondria will be degraded and recycled through IPTC-induced mitophagy. 3D surface plot of the mitochondria of the cardiac cells costained with MitoProbe (red fluorescence) and MitoTracker (green fluorescence) subjected to H/R in the absence (D) and presence (E) of IPTC.

synergistic approach where mitophagy is coupled with enhancing mitochondrial function to counteract the detrimental effects of ischemia-reperfusion on cardiomyocytes.

In our proposed mechanism, IPTC operates within a dynamic equilibrium among its different forms, contingent upon the cell's redox status. In both regular and inflamed cells, the varying reduction rates of IPTC reflect distinct redox conditions. Notably, IPTC rapidly shifts to its reduced hydroxylamine form in inflamed hypoxic cells, while in well-oxygenated cardiomyocytes, it remains in its oxidized nitroxide form. This unique self-replenishing feature suggests a continuous supply of antioxidant capabilities within cells. The reversible one-electron transfer reactions inherent to IPTC facilitate the ongoing balancing of redox activities,

https://doi.org/10.1021/acsomega.4c02725
ACS Omega 2024, 9, 39401−39418

promoting the repair of damage and mitophagy of severely impaired mitochondria within a stable redox milieu. This mechanism of action of IPTC, with its ability to induce mitophagy and alleviate oxidative damage, is visually depicted in our graphical representation, Figure 8.

Including RGD peptides in IPTC offers additional therapeutic benefits, particularly in cardiovascular interventions. RGD peptides, known for binding integrin receptors on endothelial cells and cardiomyocytes, facilitate targeted delivery of therapeutic agents to vascular and myocardial injury sites.[43,61] Numerous studies have demonstrated the efficacy of RGD-based therapies in promoting angiogenesis, enhancing myocardial repair, and improving cardiac function in preclinical models of ischemic heart disease and heart failure.[18,28,61] Thus, incorporating RGD peptides into IPTC enhances its bioavailability and facilitates targeted delivery to cardiac tissues, maximizing its therapeutic efficacy in cardiovascular diseases. Our unpublished data further explores IPTC's efficacy in a rat arterial thrombosis model and its activity in ADP- or PAF-induced in vitro platelet aggregation assays, indicating potential antithrombotic activity. Moreover, we have observed the beneficial effects of IPTC on ischemia-reperfusion-induced cardiac infarct size and oxidative changes in an in vivo rat model. These findings will be detailed in a separate manuscript.

5. CONCLUSIONS

In conclusion, our study highlights IPTC's distinctive role as both an antioxidant and a promoter of mitophagy, offering a novel strategy for cardioprotection. By fostering protective mitophagy and inhibiting mPTP opening during reoxygenation, IPTC significantly reduces mtROS production and safeguards mitochondrial integrity in H9C2 cells subjected to H/R protocols.

These findings underscore IPTC's potential as a promising therapeutic candidate for addressing mitochondrial dysfunction and oxidative stress in ischemic conditions. Despite the limitation of directly visualizing IPTC's interaction with mitochondria, our comprehensive insights deepen the understanding of its mechanisms in mitigating I/R injury.

Moreover, IPTC's profound cytoprotective mechanisms, including its superior antioxidant properties compared to traditional antioxidants, make it an effective agent in preserving cell viability and mitochondrial function in cardiomyocyte models. Its ability to maintain mitochondrial structure, promote efficient energy production, and induce protective mitophagy underscores its role in enhancing cellular resilience against I/R injury.

By preventing the onset of cell death pathways through mPTP inhibition during critical reoxygenation phases, IPTC offers promise for improving outcomes in myocardial infarction and similar cardiac conditions. IPTC emerges as a multifaceted therapeutic candidate, addressing the complex challenges of I/R injury through its antioxidative, cytoprotective, and cell-preserving actions. Thus, it presents a novel approach to enhance cardiomyocyte survival and facilitate patient recovery in ischemic stress scenarios.

6. LIMITATIONS

One limitation of our study is our inability to use commercial ROS probes to validate IPTC's ability to scavenge ROS in mitochondria. Currently, no commercially available fluorescent probes are specifically designed to detect mitochondrial ROS generation comprehensively.

While several commercially available fluorescent probes for ROS detection, such as DCFDA and DHE, exist, they lack specificity for mitochondrial ROS detection. Additionally, probes like MitoSOX, while capable of detecting mitochondrial superoxide ions, have limitations in detecting other ROS species generated within mitochondria.

Furthermore, the fluorescence emitted by MitoSOX Red is influenced by various factors, including experimental conditions and cellular environment, introducing variability between experiments.[62,63] The challenges in accurately assessing mtROS generation using commercial probes have been extensively discussed in the literature.[55,56] Researchers have highlighted the need to develop more specific probes tailored for mitochondrial ROS detection to overcome this limitation.

Given the current limitations in available fluorescent probes, we cannot conduct additional experiments using commercial ROS probes to validate IPTC's ability to scavenge ROS within mitochondria. Nevertheless, we remain dedicated to exploring alternative methodologies and strategies to elucidate further the mechanisms underlying IPTC's antioxidative effects in future studies.

Another aspect to consider is whether IPTC's effectiveness in alleviating H/R injury in H9C2 cells extends to mitigating ROS originating from organelles other than mitochondria. This is crucial for a comprehensive understanding of IPTC's antioxidative mechanisms.

Mitochondria are recognized as the primary source of ROS within cells. They are particularly susceptible to ROS-induced damage due to their involvement in aerobic respiration and electron transport chain activity. While ROS can be generated in various cellular compartments, including the endoplasmic reticulum and peroxisomes, mitochondria are notably vulnerable.

Numerous studies highlight the pivotal role of mitochondria in ROS-mediated cellular damage and the importance of targeting mtROS in oxidative stress-related pathologies. Strategies focused on modulating mtROS have thus emerged as promising therapeutic approaches.[64,65]

However, it is essential to acknowledge the absence of commercially available fluorescent probes specifically tailored to detect ROS generation from organelles other than mitochondria exclusively. Consequently, while the potential of IPTC in mitigating H/R injury by targeting ROS from other organelles is intriguing, directly assessing and quantifying ROS generation from specific organelles apart from mitochondria using current methods is challenging. Future investigations employing advanced imaging techniques, organelle-specific ROS probes, and innovative methodologies may provide further insights into IPTC's role in modulating ROS dynamics across different cellular compartments.

Thus, while mitochondria are the primary site of ROS generation and targets within cells, elucidating IPTC's specific contribution in mitigating ROS from other organelles necessitates tailored experimental approaches and innovative methodologies.

Additionally, it is worth mentioning that while our study on the cytoprotective properties of IPTC reveals its potential in mitigating I/R injury, certain limitations accompany our current research efforts. Using PC 12 cell lines and H9C2 cardiomyoblasts, though invaluable for understanding IPTC's

https://doi.org/10.1021/acsomega.4c02725
ACS Omega 2024, 9, 39401−39418

biochemical impact under controlled conditions, might only partially capture the complexity of in vivo cardiac physiology. While effective in mimicking certain aspects of oxidative stress and mitochondrial dynamics, the cellular models cannot replicate the intricate interplay of cells, tissues, and organ systems in a living organism. Consequently, the extrapolation of these in vitro findings to clinical scenarios should be cautiously approached until comprehensive in vivo studies are validated.

Moreover, the study's focus on the antioxidative and mitophagy-inducing properties of IPTC, though critical, overlooks other potential cellular pathways and mechanisms that IPTC might influence or contribute to its overall protective effects in I/R injury. The interaction of IPTC with different cellular targets, its long-term effects on cardiac function, and possible off-target effects remain areas that warrant further investigation. Additionally, the therapeutic window and optimal dosing of IPTC for maximal protection against I/R injury without adverse effects are yet to be defined. These gaps in our understanding highlight the need for continued research, encompassing broader mechanistic studies and translational research to evaluate the efficacy, safety, and practical application of IPTC in treating cardiac I/R injury.

AUTHOR INFORMATION

Corresponding Authors

Zhiying Shan − *Department of Kinesiology and Integrative Physiology, Health Research Institute and Health Research Institute, Michigan Technological University, Houghton, Michigan 49931, United States;* orcid.org/0000-0002-9763-205X; Email: zhiyings@mtu.edu

Lanrong Bi − *Department of Chemistry, Michigan Technological University, Houghton, Michigan 49931, United States; Health Research Institute, Michigan Technological University, Houghton, Michigan 49931, United States;* orcid.org/0000-0001-6624-8314; Email: lanrong@mtu.edu

Authors

Shanshan Hou − *Department of Chemistry, Michigan Technological University, Houghton, Michigan 49931, United States*

Xin Yan − *Department of Chemistry, Michigan Technological University, Houghton, Michigan 49931, United States*

Xiang Gao − *Department of Chemistry, Michigan Technological University, Houghton, Michigan 49931, United States*

Steffen Jockusch − *Center of Photochemical Sciences, Bowling Green State University, Bowling Green, Ohio 43403, United States;* orcid.org/0000-0002-4592-5280

K. Michael Gibson − *Department of Pharmacotherapy, College of Pharmacy and Pharmaceutical Sciences, Washington State University, Spokane, Washington 99202, United States*

Complete contact information is available at: https://pubs.acs.org/10.1021/acsomega.4c02725

Author Contributions

Conceptualization L.B. and Z.S; methodology and investigation, L.B.; X.G.; X.Y. S.H.; S.J.; X.G.; X.Y.; S. J., and K.G.M. Z.S.; data analysis, Z. S.; L.B.; X.G.; X.Y.; S. H.; S. J., and K.G.M. writing, reviewing and editing; Z.S. and L.B.; funding acquisition. All authors have read and agreed to the published version of the manuscript.

Funding

NIH grants R01HL163159 (Z.S.), the American Heart Association (AHA) grants 1807047 (L.B.), and NIHR15 EB035866−01 (L.B and Z.S).

Notes

The authors declare no competing financial interest.

ACKNOWLEDGMENTS

We sincerely thank the NIH and AHA for their generous financial support and Dr. Rick Koubek's encouragement and unwavering support throughout our project.

REFERENCES

(1) Sánchez-Hernández, C. D.; Torres-Alarcon, L. A.; Gonzalez-Cortes, A.; Peon, A. N. Ischemia/Reperfusion Injury: Pathophysiology, Current Clinical Management, and Potential Preventive Approaches. *Mediators Inflammation* **2020**, *2020*, No. 8405370.

(2) Zhang, M.; Liu, Q.; Meng, H.; Duan, H.; Liu, X.; Wu, J.; Gao, F.; Wang, S.; Tan, R.; Yuan, J. Ischemia-reperfusion injury: molecular mechanisms and therapeutic targets. *Signal Transduction Targeted Ther.* **2024**, *9* (1), No. 12.

(3) Xiang, M.; Lu, Y.; Xin, L.; Gao, J.; Shang, C.; Jiang, Z.; Lin, H.; Fang, X.; Qu, Y.; Wang, Y.; Shen, Z.; Zhao, M.; Cui, X. Role of Oxidative Stress in Reperfusion following Myocardial Ischemia and Its Treatments. *Oxid. Med. Cell. Longevity* **2021**, *2021*, No. 6614009.

(4) Jurcau, A.; Simion, A. Neuroinflammation in Cerebral Ischemia and Ischemia/Reperfusion Injuries: From Pathophysiology to Therapeutic Strategies. *Int. J. Mol. Sci.* **2022**, *23* (1), No. 14, DOI: 10.3390/ijms23010014.

(5) Dery, K. J.; Kupiec-Weglinski, J. W. New insights into ischemia-reperfusion injury signaling pathways in organ transplantation. *Curr. Opin. Organ Transplant.* **2022**, *27* (5), 424−433.

(6) Kulek, A. R.; Anzell, A.; Wider, J. M.; Sanderson, T. H.; Przyklenk, K. Mitochondrial Quality Control: Role in Cardiac Models of Lethal Ischemia-Reperfusion Injury. *Cells* **2020**, *9* (1), No. 214, DOI: 10.3390/cells9010214.

(7) Wang, M.; Pan, W.; Xu, Y.; Zhang, J.; Wan, J.; Jiang, H. Microglia-Mediated Neuroinflammation: A Potential Target for the Treatment of Cardiovascular Diseases. *J. Inflammation Res.* **2022**, *15*, 3083−3094.

(8) Cardinal, H.; Dieude, M.; Hebert, M. J. Endothelial Dysfunction in Kidney Transplantation. *Front. Immunol.* **2018**, *9*, No. 1130.

(9) Dong, Y.; Chen, H.; Gao, J.; Liu, Y.; Li, J.; Wang, J. Molecular machinery and interplay of apoptosis and autophagy in coronary heart disease. *J. Mol. Cell. Cardiol.* **2019**, *136*, 27−41.

(10) Liggett, J. R.; Kang, J.; Ranjit, S.; Rodriguez, O.; Loh, K.; Patil, D.; Cui, Y.; Duttargi, A.; Nguyen, S.; He, B.; Lee, Y.; Oza, K.; Frank, B. S.; Kwon, D.; Li, H. H.; Kallakury, B.; Libby, A.; Levi, M.; Robson, S. C.; Fishbein, T. M.; Cui, W.; Albanese, C.; Khan, K.; Kroemer, A. Oral N-acetylcysteine decreases IFN-gamma production and ameliorates ischemia-reperfusion injury in steatotic livers. *Front. Immunol.* **2022**, *13*, No. 898799.

(11) Olesen, H. Ø.; Pors, S. E.; Jensen, L. B.; Gronning, A. P.; Lemser, C. E.; Nguyen Heimburger, M. T. H.; Mamsen, L. S.; Getreu, N.; Christensen, S. T.; Andersen, C. Y.; Kristensen, S. G. N-acetylcysteine protects ovarian follicles from ischemia-reperfusion injury in xenotransplanted human ovarian tissue. *Hum. Reprod.* **2021**, *36* (2), 429−443.

(12) Wallert, M.; Ziegler, M.; Wang, X.; Maluenda, A.; Xu, X.; Yap, M. L.; Witt, R.; Giles, C.; Kluge, S.; Hortmann, M.; Zhang, J.; Meikle, P.; Lorkowski, S.; Peter, K. alpha-Tocopherol preserves cardiac function by reducing oxidative stress and inflammation in ischemia/reperfusion injury. *Redox Biol.* **2019**, *26*, No. 101292.

(13) Zakharova, I. O.; Bayunova, L. V.; Zorina, I. I.; Sokolova, T. V.; Shpakov, A. O.; Avrova, N. F. Insulin and alpha-Tocopherol Enhance

the Protective Effect of Each Other on Brain Cortical Neurons under Oxidative Stress Conditions and in Rat Two-Vessel Forebrain Ischemia/Reperfusion Injury. *Int. J. Mol. Sci.* **2021**, *22* (21), No. 11768, DOI: 10.3390/ijms222111768.
(14) Benoit, L.; Dieu, A.; Foguenne, M.; Bonaccorsi-Riani, E. Experimental and Clinical Aspects of Sevoflurane Preconditioning and Postconditioning to Alleviate Hepatic Ischemia-Reperfusion Injury: A Scoping Review. *Int. J. Mol. Sci.* **2023**, *24* (3), No. 2340, DOI: 10.3390/ijms24032340.
(15) Jonker, S. J.; Menting, T. P.; Warle, M. C.; Ritskes-Hoitinga, M.; Wever, K. E. Preclinical Evidence for the Efficacy of Ischemic Postconditioning against Renal Ischemia-Reperfusion Injury, a Systematic Review and Meta-Analysis. *PLoS One* **2016**, *11* (3), No. e0150863.
(16) Karwi, Q. G.; Bice, J. S.; Baxter, G. F. Pre- and postconditioning the heart with hydrogen sulfide (H(2)S) against ischemia/reperfusion injury in vivo: a systematic review and meta-analysis. *Basic Res. Cardiol.* **2018**, *113* (1), No. 6.
(17) Ali, T.; Rahman, S. U.; Hao, Q.; Li, W.; Liu, Z.; Ali Shah, F.; Murtaza, I.; Zhang, Z.; Yang, X.; Liu, G.; Li, S. Melatonin prevents neuroinflammation and relieves depression by attenuating autophagy impairment through FOXO3a regulation. *J. Pineal Res.* **2020**, *69* (2), No. e12667.
(18) Bi, W.; Bi, L.; Cai, J.; Liu, S.; Peng, S.; Fischer, N. O.; Tok, J. B.; Wang, G. Dual-acting agents that possess free radical scavenging and antithrombotic activities: design, synthesis, and evaluation of phenolic tetrahydro-beta-carboline RGD peptide conjugates. *Bioorg. Med. Chem. Lett.* **2006**, *16* (17), 4523−4527.
(19) Bi, W.; Bi, Y.; Gao, X.; Li, P.; Hou, S.; Zhang, Y.; Bammert, C.; Jockusch, S.; Legalley, T. D.; Michael Gibson, K.; Bi, L. Indole-TEMPO conjugates alleviate ischemia-reperfusion injury via attenuation of oxidative stress and preservation of mitochondrial function. *Bioorg. Med. Chem.* **2017**, *25* (9), 2545−2568.
(20) Bi, W.; Bi, Y.; Gao, X.; Yan, X.; Zhang, Y.; Harris, J.; Legalley, T. D.; Gibson, K. M.; Bi, L. Pharmacological protection of mitochondrial function mitigates acute limb ischemia/reperfusion injury. *Bioorg. Med. Chem. Lett.* **2016**, *26* (16), 4042−4051.
(21) Bi, W.; Bi, Y.; Gao, X.; Yan, X.; Zhang, Y.; Xue, P.; Bammert, C. E.; Legalley, T. D.; Michael Gibson, K.; Bi, L.; Wang, J. X. Anti-inflammatory, analgesic and antioxidant activities of novel kyotorphin-nitroxide hybrid molecules. *Bioorg. Med. Chem. Lett.* **2016**, *26* (8), 2005−2013.
(22) Bi, W.; Bi, Y.; Li, P.; Hou, S.; Yan, X.; Hensley, C.; Bammert, C. E.; Zhang, Y.; Gibson, K. M.; Ju, J.; Bi, L. Indole Alkaloid Derivative B, a Novel Bifunctional Agent That Mitigates 5-Fluorouracil-Induced Cardiotoxicity. *ACS Omega* **2018**, *3* (11), 15850−15864.
(23) Bi, W.; Bi, Y.; Xue, P.; Zhang, Y.; Gao, X.; Wang, Z.; Li, M.; Baudy-Floc'h, M.; Ngerebara, N.; Gibson, K. M.; Bi, L. Synthesis and characterization of novel indole derivatives reveal improved therapeutic agents for treatment of ischemia/reperfusion (I/R) injury. *J. Med. Chem.* **2010**, *53* (18), 6763−6767.
(24) Bi, W.; Bi, Y.; Xue, P.; Zhang, Y.; Gao, X.; Wang, Z.; Li, M.; Baudy-Floc'h, M.; Ngerebara, N.; Gibson, K. M.; Bi, L. A new class of beta-carboline alkaloid-peptide conjugates with therapeutic efficacy in acute limb ischemia/reperfusion injury. *Eur. J. Med. Chem.* **2011**, *46* (5), 1453−1462.
(25) Bi, W.; Bi, Y.; Xue, P.; Zhang, Y.; Gao, X.; Wang, Z.; Li, M.; Baudy-Floc'h, M.; Ngerebara, N.; Li, X.; Gibson, K. M.; Bi, L. Novel beta-carboline-tripeptide conjugates attenuate mesenteric ischemia/reperfusion injury in the rat. *Eur. J. Med. Chem.* **2011**, *46* (6), 2441−2452.
(26) Bi, W.; Cai, J.; Liu, S.; Baudy-Floc'h, M.; Bi, L. Design, synthesis and cardioprotective effect of a new class of dual-acting agents: phenolic tetrahydro-beta-carboline RGD peptidomimetic conjugates. *Bioorg. Med. Chem.* **2007**, *15* (22), 6909−6919.
(27) Bi, W.; Cai, J.; Xue, P.; Zhang, Y.; Liu, S.; Gao, X.; Li, M.; Wang, Z.; Baudy-Floc'h, M.; Green, S. A.; Bi, L. Protective effect of nitronyl nitroxide-amino acid conjugates on liver ischemia-reperfusion induced injury in rats. *Bioorg. Med. Chem. Lett.* **2008**, *18* (6), 1788−1794.
(28) Bi, W.; Li, X.; Bi, Y.; Xue, P.; Zhang, Y.; Gao, X.; Wang, Z.; Li, M.; Itagaki, Y.; Bi, L. Novel TEMPO-PEG-RGDs conjugates remediate tissue damage induced by acute limb ischemia/reperfusion. *J. Med. Chem.* **2012**, *55* (9), 4501−4505.
(29) Bi, W.; Wang, F.; Bi, Y.; Wang, T.; Xue, P.; Zhang, Y.; Gao, X.; Liu, S.; Wang, Z.; Li, M.; Baudy-Floc'h, M.; Robinson, S. C.; Ngerebara, N.; Bi, L. Renal ischemia/reperfusion injury in rats is attenuated by a synthetic glycine derivative. *Eur. J. Pharmacol.* **2009**, *616* (1−3), 256−264.
(30) Zhao, M.; Bi, L.; Bi, W.; Wang, C.; Yang, Z.; Ju, J.; Peng, S. Synthesis of new class dipeptide analogues with improved permeability and antithrombotic activity. *Bioorg. Med. Chem.* **2006**, *14* (14), 4761−4774.
(31) Zhao, M.; Bi, L.; Wang, W.; Wang, C.; Baudy-Floc'h, M.; Ju, J.; Peng, S. Synthesis and cytotoxic activities of beta-carboline amino acid ester conjugates. *Bioorg. Med. Chem.* **2006**, *14* (20), 6998−7010.
(32) Donia, T.; Gerges, M. N.; Mohamed, T. M. Anticancer Effects of Combination of Indole-3-Carbinol and Hydroxychloroquine on Ehrlich Ascites Carcinoma via Targeting Autophagy and Apoptosis. *Nutr. Cancer* **2022**, *74* (5), 1802−1818.
(33) Jiang, Y.; Yang, G.; Liao, Q.; Zou, Y.; Du, Y.; Huang, J. Indole-3-carbinol inhibits lipid deposition and promotes autophagy in hyperlipidemia zebrafish larvae. *Environ. Toxicol. Pharmacol.* **2019**, *70*, No. 103205.
(34) Budovska, M.; Michalkova, R.; Kello, M.; Vaskova, J.; Mojzis, J. Design, Synthesis and Antiproliferative Evaluation of Bis-Indole Derivatives with a Phenyl Linker: Focus on Autophagy. *Molecules* **2022**, *28* (1), No. 251, DOI: 10.3390/molecules28010251.
(35) Wu, J.; Bai, Y.; Wang, Y.; Ma, J. Melatonin and regulation of autophagy: Mechanisms and therapeutic implications. *Pharmacol. Res.* **2021**, *163*, No. 105279.
(36) Yilmaz, U.; Tanbek, K.; Gul, S.; Gul, M.; Koc, A.; Sandal, S. Melatonin Attenuates Cerebral Ischemia/Reperfusion Injury through Inducing Autophagy. *Neuroendocrinology* **2023**, *113* (10), 1035−1050.
(37) Zhang, Y.; Wang, Y.; Xu, J.; Tian, F.; Hu, S.; Chen, Y.; Fu, Z. Melatonin attenuates myocardial ischemia-reperfusion injury via improving mitochondrial fusion/mitophagy and activating the AMPK-OPA1 signaling pathways. *J. Pineal Res.* **2019**, *66* (2), No. e12542.
(38) Ali, N. S.; Dar, B. A.; Pradhan, V.; Farooqui, M. Chemistry and biology of indoles and indazoles: a mini-review. *Mini-Rev. Med. Chem.* **2013**, *13* (12), 1792−1800.
(39) Kaushik, N. K.; Kaushik, N.; Attri, P.; Kumar, N.; Kim, C. H.; Verma, A. K.; Choi, E. H. Biomedical importance of indoles. *Molecules* **2013**, *18* (6), 6620−6662.
(40) Hersel, U.; Dahmen, C.; Kessler, H. RGD modified polymers: biomaterials for stimulated cell adhesion and beyond. *Biomaterials* **2003**, *24* (24), 4385−4415.
(41) Hostetter, M. K. RGD-mediated adhesion in fungal pathogens of humans, plants and insects. *Curr. Opin. Microbiol.* **2000**, *3* (4), 344−348.
(42) Javid, H.; Oryani, M. A.; Rezagholinejad, N.; Esparham, A.; Tajaldini, M.; Karimi-Shahri, M. RGD peptide in cancer targeting: Benefits, challenges, solutions, and possible integrin-RGD interactions. *Cancer Med.* **2024**, *13* (2), No. e6800.
(43) Kearns, S.; Dawson, R., Jr.Cytoprotective effect of taurine against hypochlorous acid toxicity to PC12 cells. In *Taurine 4: Taurine and Excitable Tissues*, Advances in Experimental Medicine and Biology; Springer, 2002; Vol. *483*, pp 563−570.
(44) Yapici, N. B.; Jockusch, S.; Moscatelli, A.; Mandalapu, S. R.; Itagaki, Y.; Bates, D. K.; Wiseman, S.; Gibson, K. M.; Turro, N. J.; Bi, L. New rhodamine nitroxide based fluorescent probes for intracellular hydroxyl radical identification in living cells. *Org. Lett.* **2012**, *14* (1), 50−53.
(45) Denizot, F.; Lang, R. Rapid colorimetric assay for cell growth and survival. Modifications to the tetrazolium dye procedure giving

improved sensitivity and reliability. *J. Immunol. Methods* **1986**, *89* (2), 271−277.
(46) He, Y.; Li, C.; Ma, Q.; Chen, S. Esculetin inhibits oxidative stress and apoptosis in H9c2 cardiomyocytes following hypoxia/reoxygenation injury. *Biochem. Biophys. Res. Commun.* **2018**, *501* (1), 139−144.
(47) Qiu, Z.; He, Y.; Ming, H.; Lei, S.; Leng, Y.; Xia, Z. Y. Lipopolysaccharide (LPS) Aggravates High Glucose- and Hypoxia/Reoxygenation-Induced Injury through Activating ROS-Dependent NLRP3 Inflammasome-Mediated Pyroptosis in H9C2 Cardiomyocytes. *J. Diabetes Res.* **2019**, *2019*, No. 8151836.
(48) Sun, M. Y.; Ma, D. S.; Zhao, S.; Wang, L.; Ma, C. Y.; Bai, Y. Salidroside mitigates hypoxia/reoxygenation injury by alleviating endoplasmic reticulum stress-induced apoptosis in H9c2 cardiomyocytes. *Mol. Med. Rep.* **2018**, *18* (4), 3760−3768.
(49) Yao, H.; Xie, Q.; He, Q.; Zeng, L.; Long, J.; Gong, Y.; Li, X.; Li, X.; Liu, W.; Xu, Z.; Wu, H.; Zheng, C.; Gao, Y. Pretreatment with Panaxatriol Saponin Attenuates Mitochondrial Apoptosis and Oxidative Stress to Facilitate Treatment of Myocardial Ischemia-Reperfusion Injury via the Regulation of Keap1/Nrf2 Activity. *Oxid. Med. Cell. Longevity* **2022**, *2022*, No. 9626703.
(50) Zhang, Y. N.; Pang, Y. X.; Liu, D. W.; Hu, H. J.; Xie, R. Q.; Cui, W. JMJD5 attenuates oxygen-glucose deprivation and reperfusion-induced injury in cardiomyocytes through regulation of HIF-1alpha-BNIP3. *Kaohsiung J. Med. Sci.* **2022**, *38* (1), 38−48.
(51) Tambe, P. K.; Qsee, H. S.; Bharati, S. Mito-TEMPO mitigates 5-fluorouracil-induced intestinal injury via attenuating mitochondrial oxidative stress, inflammation, and apoptosis: an in vivo study. *Inflammopharmacology* **2023**, *31* (4), 2091−2102.
(52) Yang, S. G.; Bae, J. W.; Park, H. J.; Koo, D. B. Mito-TEMPO protects preimplantation porcine embryos against mitochondrial fission-driven apoptosis through DRP1/PINK1-mediated mitophagy. *Life Sci.* **2023**, *315*, No. 121333.
(53) Zhao, M.; Wang, Y.; Li, L.; Liu, S.; Wang, C.; Yuan, Y.; Yang, G.; Chen, Y.; Cheng, J.; Lu, Y.; Liu, J. Mitochondrial ROS promote mitochondrial dysfunction and inflammation in ischemic acute kidney injury by disrupting TFAM-mediated mtDNA maintenance. *Theranostics* **2021**, *11* (4), 1845−1863.
(54) Javadov, S.; Hunter, J. C.; Barreto-Torres, G.; Parodi-Rullan, R. Targeting the mitochondrial permeability transition: cardiac ischemia-reperfusion versus carcinogenesis. *Cell Phys. Biochem.* **2011**, *27* (3−4), 179−190.
(55) Dikic, I.; Elazar, Z. Mechanism and medical implications of mammalian autophagy. *Nat. Rev. Mol. Cell Biol.* **2018**, *19* (6), 349−364.
(56) Petronilli, V.; Miotto, G.; Canton, M.; Colonna, R.; Bernardi, P.; Di Lisa, F. Imaging the mitochondrial permeability transition pore in intact cells. *Biofactors* **1998**, *8* (3−4), 263−272.
(57) Alves-Figueiredo, H.; Silva-Platas, C.; Lozano, O.; Vazquez-Garza, E.; Guerrero-Beltran, C. E.; Zarain-Herzberg, A.; Garcia-Rivas, G. A systematic review of post-translational modifications in the mitochondrial permeability transition pore complex associated with cardiac diseases. *Biochim. Biophys. Acta, Mol. Basis Dis.* **2021**, *1867* (1), No. 165992.
(58) Javadov, S.; Karmazyn, M.; Escobales, N. Mitochondrial permeability transition pore opening as a promising therapeutic target in cardiac diseases. *J. Pharmacol. Exp. Ther.* **2009**, *330* (3), 670−678.
(59) Mendoza, A.; Patel, P.; Robichaux, D.; Ramirez, D.; Karch, J. Inhibition of the mPTP and Lipid Peroxidation Is Additively Protective Against I/R Injury. *Circ. Res.* **2024**, *134* (10), 1292−1305.
(60) Ong, S. B.; Dongworth, R. K.; Cabrera-Fuentes, H. A.; Hausenloy, D. J. Role of the MPTP in conditioning the heart - translatability and mechanism. *Br. J. Pharmacol.* **2015**, *172* (8), 2074−2084.
(61) Zhang, L.; Li, Z.; Ye, X.; Chen, Z.; Chen, Z. S. Mechanisms of thrombosis and research progress on targeted antithrombotic drugs. *Drug Discovery Today* **2021**, *26* (10), 2282−2302.
(62) Murphy, M. P.; Bayir, H.; Belousov, V.; Chang, C. J.; Davies, K. J. A.; Davies, M. J.; Dick, T. P.; Finkel, T.; Forman, H. J.; Janssen-Heininger, Y.; Gems, D.; Kagan, V. E.; Kalyanaraman, B.; Larsson, N. G.; Milne, G. L.; Nystrom, T.; Poulsen, H. E.; Radi, R.; Van Remmen, H.; Schumacker, P. T.; Thornalley, P. J.; Toyokuni, S.; Winterbourn, C. C.; Yin, H.; Halliwell, B. Guidelines for measuring reactive oxygen species and oxidative damage in cells and in vivo. *Nat. Metab.* **2022**, *4* (6), 651−662.
(63) Zielonka, J.; Kalyanaraman, B. Hydroethidine- and MitoSOX-derived red fluorescence is not a reliable indicator of intracellular superoxide formation: another inconvenient truth. *Free Radical Biol. Med.* **2010**, *48* (8), 983−1001.
(64) Adlam, V. J.; Harrison, J. C.; Porteous, C. M.; James, A. M.; Smith, R. A.; Murphy, M. P.; Sammut, I. A. Targeting an antioxidant to mitochondria decreases cardiac ischemia-reperfusion injury. *FASEB J.* **2005**, *19* (9), 1088−1095.
(65) Smith, R. A.; Murphy, M. P. Animal and human studies with the mitochondria-targeted antioxidant MitoQ. *Ann. N. Y. Acad. Sci.* **2010**, *1201*, 96−103.

https://doi.org/10.1021/acsomega.4c02725
ACS Omega 2024, 9, 39401−39418